

HESFIRE: an explicit fire model for projections in the coupled Human-Earth System.

Y. Le Page¹, D. Morton², B. Bond-Lamberty¹, J.M.C. Pereira³, G. Hurtt⁴

¹Pacific Northwest National Laboratory, Joint Global Change Research Institute, University of Maryland, College Park, MD 20740, USA

²NASA Goddard Space Flight Center, Greenbelt, MD 20771, USA

³Centro de Estudos Florestais, Instituto Superior de Agronomia, Universidade de Lisboa, Tapada da Ajuda, 1349-017 Lisbon, Portugal

⁴Department of Geographical Sciences, University of Maryland, College Park, MD 20740, USA

Corresponding author: Yannick Le Page, Yannick.LePage@pnnl.gov

Abstract

Vegetation fires are a major driver of ecosystem dynamics and greenhouse gas emissions. Potential changes in fire activity under future climate and land use scenarios thus have important consequences for human and natural systems. Anticipating these consequences relies first on a realistic model of fire activity (e.g. fire incidence and inter-annual variability) and second on a model accounting for fire impacts (e.g. mortality and emissions). Key opportunities remain to develop the capabilities of fire activity models, which include quantifying the influence of poorly understood fire drivers, modeling the occurrence of large, multi-day fires - which have major impacts – and evaluating the fire driving assumptions and parameterization with observation data. Here, we describe the HESFIRE model, which integrates the influence of weather, vegetation characteristics, and human activities on fires in a standalone framework, with a particular emphasis on keeping model assumptions consistent with fire ecology, such as allowing fires to spread over consecutive days. A subset of the model parameters was calibrated through an optimization procedure using observation data to enhance our understanding of regional drivers of fire activity and improve the performance of the model on a global scale. Modeled fire activity showed

1 reasonable agreement with observations of burned area, fire seasonality and inter-annual
2 variability in many regions, including for spatial and temporal domains not included in the
3 optimization procedure. Significant discrepancies are investigated, most notably regarding
4 fires in boreal regions, in xeric ecosystems, and fire size distribution. We highlight the
5 capabilities of HESFIRE and its optimization procedure to analyze the sensitivity of fire
6 activity, and to provide fire projections in the coupled Human-Earth System at regional and
7 global scale. These capabilities and their detailed evaluation also provide a solid foundation
8 for integration within a vegetation model to represent fire impacts on vegetation dynamics
9 and emissions.

10

11 **Keywords:** vegetation fire model, coupled human-Earth system, fire ignition/spread/termination,
12 model optimization, model evaluation.

13

14 1. Introduction

15 [1] The human population has more than doubled in the past 50 years, expanding the scale and
16 diversity of changes in the Earth system from anthropogenic activity. The build-up of greenhouse
17 gases in the atmosphere, as well as the degradation and conversion of natural lands, have major
18 consequences for future climate, natural ecosystems, and human societies (Parry, 2007; Stocker et al.,
19 2013). The interactions between human and natural systems are complex, yet observational data,
20 field experiments, and various types of models continue to elucidate key linkages among climate
21 variability, ecosystem function, and anthropogenic activities. This knowledge is essential to anticipate
22 potential changes under future conditions and to design adaptation or mitigation strategies that
23 promote the sustainability of the coupled Human-Earth system.

24 [2] One of these interactive processes linking human activities and natural ecosystems is fire
25 (Bowman et al., 2009). Humans exert considerable influence over global fire activity (Le Page et al.,
26 2010a); fire-driven deforestation accounts for an estimated 20% of the increase in atmospheric CO₂

1 from human activities since preindustrial times (Bowman et al., 2011; van der Werf et al., 2010). Fire
2 activity depends on a range of drivers covering three major components of the Human-Earth
3 System: the atmosphere (e.g. weather conditions), the terrestrial biosphere (e.g. fuel loads) and
4 anthropogenic activities (e.g. land-use fires and fire suppression). The interaction among these
5 drivers determines global fire activity, as illustrated in 1997-1998 when a strong El Niño led to
6 extreme fire events around the world (Le Page et al., 2008), including unprecedented fires in
7 peatlands and forests of Indonesia where human-caused fires emitted an estimated 13 to 40% of the
8 world's annual fossil fuel emissions (Page et al., 2002).

9 [3] Future fire activity and impacts thus depends on the synergistic interactions between these
10 drivers, and on fire-mediated feedbacks in the Earth system. In boreal regions, recent increases in
11 fire activity are consistent with warming and drying trends that favor fire occurrence (Gillett et al.,
12 2004; Goetz et al., 2005). Projected increases in fire activity from climate change in other ecosystems
13 range from a moderate decrease to a 5-fold increase depending on characteristics of the climate
14 projections and modeling frameworks (e.g. Flannigan et al., 2009; Liu et al., 2010; Soares-Filho et al.,
15 2012). Studies that consider both climatic and anthropogenic drivers highlight the sensitivity of
16 future fire activity to societal developments, including fire suppression and fire-driven deforestation
17 of natural ecosystems for agricultural expansion (Cardoso et al., 2003; Keeley and Fotheringham,
18 2003; Kloster et al., 2012; Le Page et al., 2010b). In return, altered fire activity may amplify or
19 moderate climate change via global greenhouse gas emissions and local albedo changes (Liu et al.,
20 2013; Randerson et al., 2006). Net changes in carbon emissions from disturbances, including fires,
21 constitute a major uncertainty for climate change adaptation and mitigation assessments: any
22 unforeseen increase in greenhouse gas emissions from fire would require an adaptive mitigation
23 effort to achieve a predefined climate target (Le Page et al., 2013; Running, 2008).

1 [4] Modeling changes in fire activity under future climate, policy, and land use scenarios requires
2 a framework with a broad range of variables (Pechony and Shindell, 2009) and a good understanding
3 of the influence of these variables for model parameterization. A range of global fire models have
4 been developed in recent decades, each with a different focus (e.g. Arora and Boer, 2005; Li et al.,
5 2013; Pfeiffer et al., 2013; Prentice et al., 2011; Thonicke et al., 2001, 2010). Among these examples,
6 SPITFIRE (Thonicke et al., 2010) is a process-based fire model coupled to a vegetation model
7 explicitly representing many physical properties of fire behavior providing great capabilities
8 regarding fire spread, fire intensity and fire impacts (damage, mortality, emissions). The model
9 developed by Li et al. (2013) has a particular emphasis on depicting anthropogenic ignitions, with
10 good performances regarding global patterns of burned area.

11 [5] One key prospect to build upon existing work, as mentioned by Thonicke et al. (2010), is to
12 develop the capability for modeling fire spread over consecutive days. This capability has been
13 reported in one global fire model focusing on pre-industrial era fires (Pfeiffer et al., 2013). In many
14 ecosystems, multi-day fires are a major driver of the overall fire activity. In boreal regions, dry-spells
15 and heat-waves in days and weeks following ignition enable the growth of large fires (Abatzoglou
16 and Kolden, 2011), and although those burning over 200ha represent a minor fraction of all fires,
17 they typically account for 90+% of the total area burned (Stocks et al., 2002). In tropical forests,
18 large-scale climate anomalies allow individual fires to over the course of several weeks, including
19 areas further away from the forest edge where ignition typically occurs (Morton et al., 2013). Similar
20 findings have been reported for temperate regions, including in Mediterranean ecosystems (Pereira
21 et al., 2005; Westerling et al., 2004). Modeling fire-climate interactions therefore requires careful
22 attention to the duration of fire weather events.

1 [6] Another opportunity for fire modeling research is model parameterization and their
2 evaluation. Many early models had to extrapolate findings from local studies or to simplify key
3 drivers of fire activity when information of some components was unavailable (e.g. ignitions
4 independent of anthropogenic activities). Recently, model calibration has been applied to one
5 (Thonicke et al., 2010) or a few (Li et al., 2013) parameters. Expanding this approach to additional
6 parameters in a model with realistic assumptions on key aspects of fire ecology could yield relevant
7 insights on fire drivers. Subsequent model evaluation is essential to assess our confidence in fire
8 projections, especially regarding fire activity - which global spatio-temporal patterns are relatively
9 well characterized by observation data (Mouillot et al., 2014) – because depicting patterns of fire
10 activity and their sensitivity to fire drivers is a pre-requisite to project realistic fire impacts.
11 Evaluating fire models is challenging when they are embedded within vegetation models however,
12 because vegetation distribution strongly affects fire dynamics (Scott and Burgan, 2005), and if
13 inaccurate (e.g. figure 7 in Sitch et al., 2003, figure 2 in Cramer et al., 2001), may lead to unrealistic
14 fire projections for reasons unrelated to the fire parameterization.

15 [7] This paper describes the development of the HESFIRE model (Human-Earth System
16 FIRE), aiming to improve our understanding of current fire activity and our capacity to anticipate its
17 evolution with future environmental and societal changes. HESFIRE is first developed as a
18 standalone model, i.e. not integrated within a dynamic vegetation model. The major emphasis of this
19 research is to outline the model structure and apply an optimization procedure to explore some of
20 the research opportunities mentioned above. Our analysis has three main objectives: 1) explicit
21 representation of fire ignition, spread, and termination, with realistic assumptions regarding fire
22 ecology (e.g. multi-day fires); 2) consideration of atmospheric, terrestrial, and anthropogenic drivers
23 in order to represent synergistic effects among changes in climate, vegetation, and human activity—
24 key steps towards the implementation of the fire model within Human- and Earth-system models;

1 and 3) model optimization and evaluation to improve our understanding of constraints on global fire
2 activity and to quantify uncertainties of future fire activity projections.

3 **2. Methods**

4 **2.1. Model overview**

5 [8] The structure of HESFIRE was designed to satisfy objectives 1 & 2 (realistic assumptions
6 and ease of integration to vegetation and integrated assessment models), and some of its parameters
7 were optimized to estimate the quantitative role of poorly understood drivers and to maximize the
8 agreement between modeled and observed fire regimes (objective 3). The model focuses on fires in
9 natural ecosystems: deforestation and agricultural fires are dependent on very different dynamics
10 (controlled spread, pile burning) and thus only considered as a source of ignition for escaped fires.

11 [9] The model is organized in three parts, with specific drivers for fire ignition, spread, and
12 termination (Figure 1):

13 - Fire ignitions. Natural ignitions are a function of cloud-to-ground lightning strikes and a
14 probability of ignition per strike. Human ignitions reflect agricultural and ecosystem
15 management as a function of land use density and national Gross Domestic Product (GDP).

16 - Fire spread. Fire spread rate is a function of weather conditions (relative humidity,
17 temperature, wind speed), soil moisture, and fuel structure categories (forest, shrub, grass).

18 - Fire termination. Four factors control the termination of fires: weather conditions, fuel
19 availability, landscape fragmentation, and fire suppression efforts (a function of land use,
20 GDP and fire suppressibility).

1 [10] To account for the diurnal variability in fire spread and termination (see introduction), every
2 fire is tracked individually with a 12-hour timestep. The analyses presented in this paper were
3 conducted with model runs at a resolution of 1-degree.

4 [11] HESFIRE was coded in Python 2.7 and is freely available at
5 <https://github.com/HESFIRE/model> (Note: open source licensing in process at the time of
6 writing). The optimization procedure is included in the code.

7 **2.2. Model description**

8 [12] The full list of parameters is described in Table 1. The following sections detail the fire
9 ignition, spread and termination modules.

10 **2.2.1. Fire ignitions**

11 [13] Fires may occur due to natural ignitions (NAT_{ign}) and human ignitions (LU_{ign}):

$$N_{fires} = NAT_{ign} + LU_{ign} \quad \text{Eq. 1}$$

12

13 To introduce some of the stochasticity associated with fires, N_{fires} represents the expected
14 realization of a Bernoulli trial ($n=1000$), and the final number of ignitions is computed following
15 the actual trial.

16 **2.2.1.1. Natural ignitions**

17 [14] Lightning strikes are the most frequent source of natural ignitions. Lightning ignitions are
18 highly stochastic because of the localized occurrence of convective storms, variability in the
19 frequency of cloud-to-ground lightning, and coincident rainfall which can terminate ignited fires

1 before substantial spread occurs (see review in Podur et al., 2003). In HESFIRE, natural ignitions
2 are the product of cloud-to-ground lightning strikes, the probability of ignition from lightning, and
3 the fractional cover of flammable vegetation in a given grid cell:

$$NAT_{ign} = CG_{flashes} \times CG_{ignp} \times (1 - Frag_n) \quad \text{Eq. 2}$$

4

5 Where $CG_{flashes}$ is the number of cloud-to-ground lightning strikes, CG_{ignp} is the lightning ignition
6 probability determined through the optimization procedure (see Sect. 2.3), and $Frag_n$ (fragmentation)
7 the fraction of the grid-cell that cannot sustain a fire (non-natural land or not enough fuel, see later).

8 **2.2.1.2. Anthropogenic ignitions**

9 [15] Humans are the dominant source of fire ignition in most temperate and tropical ecosystems.
10 Ignitions from human activities include fires for agriculture and ecosystem management,
11 deforestation for agricultural expansion, accidental fires, and arson. Fire usage varies across
12 countries, climate zones, and land use practices (Korontzi et al., 2006; Le Page et al., 2010a), and this
13 diversity of human activity cannot be fully captured with current knowledge and data. However,
14 wealth is an important driver of fire use in agricultural settings, since fire is typically the least costly
15 tool to clear natural vegetation, control pests, or increase soil fertility (Laris, 2002; Thrupp et al.,
16 1997). Thus we represent anthropogenic ignitions as a function of land use intensity and national
17 GDP, where higher fractional land use and lower GDP increase anthropogenic fire ignitions. Similar
18 to the approach used in the SPITFIRE model (Thonicke et al., 2010), we assume that initial
19 settlements bring more ignitions relative to additional ones:

$$Humign = (1 - GDP_n)^{GDP_{exp}} \times \int_0^{LU} LU_{ign} \times LU \times (1 - LU_n)^{LU_{exp}} \quad \text{Eq. 3}$$

1
2 where GDP_n is the normalized Gross Domestic Product per capita (from 0\$ to 60000\$), GDP_{exp} the
3 associated shape parameter, LU_{ign} is the number of ignitions per km^2 of land use, LU the land use
4 area in the grid-cell considered, and LU_{exp} the shape parameter controlling the decrease in the
5 amount of additional ignitions with incremental land use. LU_n is the normalized land use fraction of
6 the grid-cell, from 0 to 0.1 only. Applying a wider normalization range systematically led to very high
7 values of the optimized parameter LU_{exp} , pointing to a rapid saturation of human ignitions with land
8 use density. LU_{ign} and GDP_{exp} were also determined through our optimization procedure. Eq. 3
9 conveys the following fire driving mechanisms:

10 - Human ignitions increase with human occupation of the landscape, but saturate once 10% of
11 the landscape is occupied.

12 - Fire use for land use management depends on the regional GDP, with maximum fire use in
13 the poorest regions, and virtually no fire use at all for regions beyond 60000\$/capita. Only
14 one country (Qatar) has a GDP beyond this range in the data. In the future, more countries
15 are expected to have a GDP over 60000\$/capita, and thus would not have any human
16 ignitions (see discussion).

17 **2.2.2. Fire spread**

18 [16] The rate of fire spread is modeled for three broad vegetation types - forest, shrub, and grass
19 - and varies as a function of relative humidity, soil moisture, temperature, wind speed, and fuel

1 structure. Maximum fire spread rates are constrained by observations (Scott and Burgan, 2005):
 2 0.28m/s in forests, 1.12m/s in shrubs, and 2.79m/s in grasses. The actual rate of fire spread F_{rate} for
 3 each vegetation type is then computed:

$$F_{rate} = Max_{rate} \times \left(1 - RH_n^{RH_{exp}}\right) \times \left(1 - SW_n^{SW_{exp}}\right) \times \left(1 - T_n^{T_{exp}}\right) \times G(W) \quad \text{Eq. 4}$$

with X_n as normalized driver, e.g.:

$$\begin{aligned} \text{If } RH \leq RH_{min} \quad & RH_n = 0 \\ \text{If } RH \geq RH_{max} \quad & RH_n = 1 \\ \text{Else} \quad & RH_n = \frac{RH - RH_{min}}{RH_{max} - RH_{min}} \end{aligned} \quad \text{Eq. 5}$$

4

5 Where RH_n is the normalized relative humidity, from $RH_{min}=30\%$ to $RH_{max}=80\%$ (adapted from Li
 6 et al., 2012). SW_n and T_n are the normalized 0-10cm layer soil moisture (20-35%, used as a proxy for
 7 fuel moisture) and temperature (0°C - 30°C), as determined by simple data analysis and parameter
 8 value trials (see Table 1 and Figure S1 in supplementary material). RH_{exp} , SW_{exp} and T_{exp} are the
 9 optimized shape parameters controlling the fire-driving relationship. The influence of wind on fire
 10 spread rate, $G(W)$, is computed following the method described in (Li et al., 2012), as a function of
 11 the length-to-breadth (LB) and head-to-back (HB) ratios of a typical elliptical burned area, both of
 12 which depend on wind speed (w).

$$LB = 1 + 10 \times (1 - e^{-0.06 \times \omega}) \quad \text{Eq. 6}$$

$$HB = LB + \frac{LB + (LB^2 - 1)^{0.5}}{LB - (LB^2 - 1)^{0.5}} \quad \text{Eq. 7}$$

$$G(W) = 2 \times \frac{LB}{(1 + 1/HB)} \times 0.0455 \quad \text{Eq. 8}$$

13

1 Within a grid cell, fires are assumed to spread with equal probability to each of the three vegetation
 2 types. Their respective burned area therefore reflects their specific fire spread rates and fraction
 3 within the grid-cell. Given the large size of the model grid cells ($1^\circ \times 1^\circ$), fire spread to neighboring
 4 grid-cells is not considered.

5 **2.2.3. Termination**

6 [17] Individual, multi-day fires are modeled from ignition to termination. Fire termination may
 7 occur in 4 ways: weather conditions are no longer favorable to fire spread, the fire is stopped by
 8 landscape fragmentation, by lack of fuel, or suppressed by fire-fighting activities. Each termination
 9 pathway contributes to the overall probability of termination; fire termination is then determined by
 10 the same Bernoulli trial stochastic approach applied to fire ignitions. Fire termination is computed
 11 every 12 hours and may occur before any spread (i.e., right after ignition).

$$N_{fires_{t+1}} = N_{fires_t} \times \left\{ \frac{(1 - Fuel_{termp}) \times (1 - Frag_{termp}) \times (1 - Supp_{termp}) \times (1 - Weather_{termp})}{(1 - Supp_{termp}) \times (1 - Weather_{termp})} \right\} \quad \text{Eq. 9}$$

12 where N_{fires} is the number of active fires, $Fuel_{termp}$, $Frag_{termp}$, $Supp_{termp}$ and $Weather_{termp}$, are the probability
 13 of termination due to each factor.

14 [18] Weather-related termination occurs when fire spread rate decreases to zero, that is when RH
 15 is 80% or above, soil moisture is 35% or above, or when the temperature drops below freezing.

16 [19] Fuel load and its impact on termination is a function of the cumulative precipitation prior to
 17 the current time step, as an indicator of water limitation on fuel build-up in arid areas:

$$Fuel_{termp} = 1 - Precip_n^{Fuel_{exp}} \quad \text{Eq. 10}$$

1 where $Precip_n$ is the average precipitation from -15 to -3 months, normalized from 0.5 mm.day-1
2 ($Precipn=1$) to 3mm.day-1 ($Precipn=0$). These were chosen based on the literature (Greenville et al.,
3 2009; Van der Werf et al., 2008; Van Wilgen et al., 2004), and on simple data analysis and parameter
4 value trials (see Table 1 and Figure S1 in supplementary material). $Fuel_{exp}$ is the shape parameter,
5 determined through the optimization procedure. Note that when integrated into an ecosystem
6 model, fuel constraints can be directly inferred from vegetation, litter and soil carbon pools.

7 [20] Landscape fragmentation is computed as the fraction of the grid-cell that cannot sustain
8 natural vegetation fires (croplands, urban areas, water bodies, deserts). Burned areas also contribute
9 to fragmentation, up to 8 months after the fire, thus avoiding repeated burns within the same fire
10 season, but allowing fuel build-up for the following fire season if enough precipitation occurs (e.g. in
11 sub-Saharan Africa).

$$Frag_{termp} = Frag_n^{Fragexp} \quad \text{Eq. 11}$$

12 where $Frag_n$ is the fraction of the grid-cell that cannot sustain a fire, normalized from 0% ($Frag_n=0$)
13 to 100% ($Frag_n=1$). $Frag_{exp}$ is the shape parameter, determined through the optimization procedure.

14 [21] Fire suppression is modeled as a function of land use (human presence), GDP, and fire
15 suppressibility. This approach assumes that 1) fire suppression activities are limited in regions with
16 low GDP, and in remote areas with little land use regardless of GDP (e.g. boreal fires in Canada and
17 Alaska, bush fires in northern Australia); and 2) the more fire prone the conditions (weather, fuel),
18 the less effective fire suppression efforts are. These assumptions are embodied in the following
19 equation:

$$Supp_{term p} = (1 - (1 - LU_n^{LUSUP_{exp}}) \times (1 - GDP_n^{GDP_{exp}})) \times (1 - F_{suppressibility}) \quad \text{Eq. 12}$$

1 where LU_n is the fraction of the grid-cell with land use, normalized from 0 ($LU_n=0$) to 0.1 ($LU_n=1$),
 2 $LUSUP_{exp}$ a shape parameter controlling the increase in suppression effort with land use density,
 3 GDP_n is the normalized GDP (from 0 to 60000\$/capita), GDP_{exp} the shape parameter, and $F_{suppressibility}$
 4 a proxy for the influence of weather and fuel on easiness of suppression. $LUSUP_{exp}$ and GDP_{exp} are
 5 determined through the optimization procedure. Note that GDP_{exp} has the same value as in Eq. 3
 6 for human ignitions. GDP has a negative relationship on fires through both ignitions and
 7 suppression, leading to an under-constrained optimization if maintaining 2 separate parameters.
 8 $F_{suppressibility}$ is dependent on weather conditions and fuel, assuming lower suppressibility with windier,
 9 drier, hotter conditions and with higher fuel load:

$$F_{suppressibility} = \left(1 - RH_n^{RH_{exp}}\right) \times \left(1 - SW_n^{SW_{exp}}\right) \times \left(1 - T_n^{T_{exp}}\right) \times G(W) \times Precip_n^{Fuel_{exp}} \quad \text{Eq. 13}$$

10

11 2.3. Model optimization

12 [22] The 9 optimized parameters (Table 1) are classified in 2 categories:

13 a. Non-shape parameters (2 out of 9) account for quantitative impacts of fire drivers:
 14 the default number of human ignitions per land use area (LU_{ign}), and the probability
 15 that lightning strikes on vegetated areas ignite a fire (CG_{ign}).

1 b. Shape parameters (7 out of 9) control the shape of the relationship between a given
2 driver and fire. For example, relative humidity is assumed to limit fire spread
3 between 30% and 80%, but the linear or non-linear relationship with relative
4 humidity between 30% and 80% and fire spread is unclear. To optimize this type of
5 parameter, the variable was first normalized between 0 (RH_{min}=30%) and 1
6 (RH_{max}=80%). Then the actual impact of RH on fire spread rates was computed
7 with a shape parameter, RH_{exp} (Eq. 4).

8 [23] These shape parameters can convey a wide range of potential driving relationships (Figure
9 2). The exponential function was selected to balance gains in process understanding and costs
10 associated with computational efforts. We assumed that fires respond monotonically to all optimized
11 drivers, but acknowledge that more complex fire driving relationships cannot be accounted for here.
12 Exploring such aspects would require 2 or more parameters per driver, which would lead to
13 computational speed and convergence problems during optimization. The objective was to infer
14 general conclusions on otherwise little understood fire drivers, for which single-parameter functions
15 were well adapted.

16 [24] We used a Markov Chain Monte Carlo approach based on the Metropolis Algorithm
17 (Metropolis et al., 1953) to obtain best-fit parameter values. The algorithm generates trial sets of
18 parameters pseudo-randomly, and compares model outputs with observation data. Each trial set is
19 either accepted or rejected, and the history of acceptance and rejection guides the generation of
20 subsequent trial sets. Acceptance occurs if a trial set leads to a better fit than the current
21 parameterization. To limit the risk of convergence to local optimums, acceptance may also occur if
22 the trial set does not have a better fit, with decreasing likelihood as the difference with the best fit
23 increases. Upon acceptance (rejection), the range of possible parameter values is increased

1 (decreased) before the next trial set is generated. The algorithm typically explored hundreds to over a
2 thousand sets of trial parameter values before converging to a best fit (Figure 3).

3 [25] The optimization metric was defined to minimize classification error across 7 classes of
4 annual burned fraction (interval boundaries: 0, 1, 5, 10, 20, 35, 50+% of the grid-cell), and to
5 maximize the correlation with observed inter-annual variability. Within each class, grid-cells are
6 attributed continuous values based on linear interpolation: a grid-cell with 3% burned fraction is
7 given the value of 2.5, being in the middle of the 2nd interval boundaries. This classification approach
8 aims at capturing important changes that would have little weight on the optimization if using direct
9 burned fraction value. The difference between 3% and 4% in fire-sensitive tropical forests is
10 probably more relevant to capture than between 33 and 34% in fire-adapted grasslands of northern
11 Australia.

12 $\mathbf{Opt}_{index} =$ Eq. 14

$$\frac{\sum_{gridcell=1}^n (\mathbf{MOD}_{fclass} - \mathbf{OBS}_{fclass})^2 + \sum_{gridcell=1}^n (1 - IAV_{corrcoef}(\mathbf{MOD}, \mathbf{OBS}))}{n}$$

13 where MOD_{fclass} and OBS_{fclass} are the modeled and observed fire classification, and $IAV_{corrcoef}$ the
14 correlation coefficients for both time series, for each grid-cell.

15 [26] The optimization was performed using modeled and observed burned area over 5-years
16 (2002-2007). Fewer than 2% of all land grid-cells were used for the optimization step; these were
17 selected manually to represent the broad spectrum of fire regimes and the range of environmental
18 conditions around the world (e.g. biomes, land use density, fuel gradient in semi-arid regions, GDP,
19 see Figure S2). No grid-cells were selected from South America, in order to test the model's ability
20 to reproduce fire patterns under combinations of drivers it might not have encountered during

1 optimization. To evaluate the robustness of the algorithm convergence, we performed 20
2 optimization runs, each using different grid-cells and years. The algorithm was a very valuable tool
3 applied repeatedly throughout model development to support its design. In particular, we used it to
4 test the relevancy of additional fire driving mechanisms by quantifying the gain in the optimization
5 index, to progressively adapt non-optimized parameters (e.g. input normalization range), and to
6 compare the performance with different data sources (e.g. alternative land cover datasets).

7 **2.3.1. Model evaluation**

8 [27] We evaluated HESFIRE using satellite-derived estimates of 1) burned area and aggregate
9 characteristics of regional fire activity over a 13-years timespan (fire incidence, seasonality, inter-
10 annual variability); and 2) the regional distribution of fire size for the year 2005.

11 [28] Finally, we performed a sensitivity analysis to evaluate the influence of each model parameter
12 on the averaged annual burned area within the model. For each parameter, the model was run twice,
13 with the parameter changed to +50% and -50% of its original value while everything else was kept
14 the same. For each grid-cell, we then extracted the parameter that generated the largest change in
15 burned area. This approach has been applied in numerous modeling studies (e.g. Potter et al., 2001;
16 White et al., 2000; Zaehle and Friend, 2010; see Saltelli et al., 2000 for alternatives methods). Results of
17 the sensitivity analysis were grouped into four classes to map the spatial distribution of parameter
18 sensitivity: 1) Climate (lightning strike, RH, soil moisture and temperature parameters); 2) Fuel
19 (precipitation-based proxy); 3) Anthropogenic (ignitions and suppression parameters); 4)
20 Fragmentation (landscape fragmentation parameter).

21 **2.4. Data**

22 **2.4.1. Weather**

1 [29] We combined two data sources to estimate the spatial and temporal variability in natural
2 ignitions from lightning. The timing and location of cloud-to-ground lightning strikes is based on
3 convective precipitation (Allen and Pickering, 2002) using sub-daily convective precipitation data
4 from NCEP (see below). We then corrected biases in the spatial distribution of lightning strikes
5 identified by the authors of this method with the observed LIS/OTD climatology (Christian et al.,
6 2003), converted to cloud-to-ground lightning strikes following (Prentice and Mackerras, 1977).

7 [30] Sub-daily relative humidity, soil moisture, temperature, wind speed and convective
8 precipitation data were obtained from the NCEP reanalysis-II project (Kanamitsu et al., 2002). For
9 fuel limitation, we used monthly precipitation data from the Global Precipitation Climatology
10 Project (GPCP, Adler et al., 2003). All data were interpolated linearly from their original resolution
11 (2.5-degree for NCEP) to the model 1-degree resolution, and averaged from 6-hourly to 12-hourly.

12 **2.4.2. Land cover**

13 [31] We used the GlobCover version 2.3 land cover map (Bontemps et al., 2011) to estimate the
14 distribution of natural ecosystems and human land uses at 1-degree resolution. GlobCover data were
15 re-gridded from the original 300m resolution to 1-degree and reclassified from 22 land cover classes
16 to the 5 classes used in the model (forests, shrublands, grasslands, croplands/urban, bare
17 areas/water).

18 **2.4.3. Land use and GDP**

19 [32] Land use density was computed as the sum of crops and urban lands in the GlobCover data.
20 National GDP was inferred from the 2009 World Factbook (CIA, 2009).

21 **2.4.4. Fire activity**

1 [33] The Global Fire Emission Database (GFED, version 3, van der Werf et al., 2010) was used
2 in the optimization procedure as well as to evaluate the representation of fire incidence, seasonality
3 and inter-annual variability in HESFIRE. The regional distribution of fire was evaluated with
4 observations from the MODIS MCD45 burned area product (Roy et al., 2008). Note that both of
5 these products feature substantial uncertainties (Giglio et al., 2010, 2013; Roy et al., 2008). In the
6 case of burned area from GFED, we consider uncertainties to be roughly 25-50% based on these
7 papers and on comparison between GFED versions 2, 3 and 4.

8 **3. Results**

9 **3.1. Optimization**

10 [34] The parameters inferred by the optimization procedure are consistent with our current
11 understanding of fire drivers, and provide a quantitative estimate on otherwise poorly constrained
12 relationships. Their value, variability across the 20 optimization runs and implications for fire
13 ignition, spread and termination are presented in Figure 4 and Figure 5. In 16 out of the 20
14 optimization runs performed, the final set of parameters was relatively similar to the final model, and
15 changes in parameter values were mostly compensative of each other, especially for correlated fire
16 drivers (e.g. relative humidity and soil moisture). In four cases, the optimization procedure reached
17 an alternative configuration, with one or several parameters differing from the final parameterization
18 by a factor greater than five, and were discarded as unsuccessful parameterization, most likely getting
19 stuck at local optimums. Hereafter, we refer to the remaining 16 models to consider parameter
20 uncertainty, represented by the black lines in Figure 4 and shaded areas in Figure 5.

21 [35] For fire ignitions, the probability that lightning strikes on natural vegetation ignite a fire
22 under fire prone conditions is optimized at 6.8% (uncertainty range [2.8 to 16.6%]), comparable to
23 the value inferred from the literature used in SPITFIRE (4%, Thonicke et al., 2010). We emphasize,

1 however, that this metric is a general probability that does not depict the complex relationship
2 between cloud-to-ground lightning strikes and fire ignitions (Podur et al., 2003). Regarding
3 anthropogenic sources, the optimization procedure suggests that the number of human ignitions
4 saturates at a low landuse fraction, with any additional land use beyond 2-3% of the grid-cell area
5 having no contribution to ignitions (Figure 5a). The final number of anthropogenic ignitions further
6 depends on GDP per capita, with a nearly linear relationship Figure 5b.

7 [36] Regarding fire spread, exponents depicting the role of RH and soil moisture indicate
8 relatively linear relationships, with significant uncertainty ($RH_{exp} = 1.18$ [0.52 to 1.29]; $SW_{exp} = 1.21$
9 [0.3 to 1.44]) (Figure 5d,e). The relationship with temperature is slightly non-linear ($T_{exp} = 1.78$ [0.80
10 to 3.30]), indicating a lower impact of temperature changes towards the higher range of the influence
11 interval ([0 30°C]). Optimizing the model without the influence of temperature produced relatively
12 similar performances, except in high-latitude regions where temperature constraints encompass
13 limits on fire spread (e.g., snow cover).

14 [37] For fire termination, the anthropogenic influence indicated a rapid saturation of suppression
15 efforts with land use density ($LUSUP_{exp} = 4.08$ [1.62 to 7.18]) and maximum suppression at 0.1
16 fractional land use (Figure 5a). The influence of GDP was approximately linear ($GDP_{exp} = 1.28$
17 [0.97 to 2.24]), while the influence of landscape fragmentation was slightly non-linear ($FRAG_{exp} =$
18 1.41 [0.83 to 3.02]). The cumulative precipitation proxy for fuel load also indicated a slightly non-
19 linear relationship ($FUEL_{exp} = 1.72$ [1.62 to 3.65]). Climatic factors only operate through condition
20 thresholds (e.g. relative humidity over 80%) and were thus not optimized.

21 **3.2. Global 1997-2010 run and comparison to observation-derived data**

1 [38] The modeled and observed average annual burned fractions across the world are illustrated
2 in Figure 6. In South America, which was not part of the optimization phase, HESFIRE depicts
3 most spatial patterns as well as the actual incidence of fires, including increased fire activity
4 associated with the expansion of human activities into the Amazon basin, the competing influence
5 of the moisture gradient (Le Page et al., 2010b), and fires associated with pastures and grasslands in
6 northern Venezuela and southern Columbia. In Africa and Australia, HESFIRE generally captures
7 high fire incidence in grassland areas, although modeled spatial patterns in Africa are more uniform
8 than observations (probably due to the simple representation of fuel, see sect. 4.1.2). HESFIRE also
9 reproduces areas of moderate fire incidence in south-eastern Asia, Kazakhstan and south-western
10 Europe, and identifies strong fire gradients with decreasing fuel load across semi-arid and arid
11 regions (e.g. in Africa, central Australia), although with some limitation especially at the northern
12 edge of sub-Saharan Africa where fire incidence is over-estimated. Conversely, HESFIRE performs
13 poorly in several regions, including the pan-boreal region, at least partly due to a bias in the climate
14 and soil moisture data (see discussion), as well as Central America, Mexico, the horn of Africa and
15 some areas of the Middle East where fire incidence is over-estimated. It also under-estimates fire
16 incidence in Indonesia, where soil moisture remains beyond the fire prone threshold almost all year
17 long. Fires preferentially occur on areas with degraded forests and drained peatlands in Indonesia
18 (Page et al., 2002; Van der Werf et al., 2008), which moisture dynamics is not captured in a 2.5-
19 degree resolution dataset.

20 [39] Aggregated monthly burned area across 14 regions and their respective fire size distribution
21 are illustrated in Figure 7. The monthly time series provide insights into the performance of
22 HESFIRE on regional fire incidence, fire seasonality and inter-annual variability. Average burned
23 area in the main fire incidence regions are in agreement with the GFED database (NHAF, SHAF,

1 AUST, SHSA). Seasonality also shows a good agreement, whether regionally or at 1-degree
2 resolution (not shown). The main seasonality discrepancy occurs in sub-Saharan Africa, where the
3 model substantially delays the onset and peak of the fire season. Finally, HESFIRE performs
4 unevenly regarding inter-annual variability, with medium to high correlation to observations in some
5 tropical and temperate regions, but low or even negative correlation in boreal regions. It reproduces
6 the El Nino induced anomaly in Indonesia in 1997-1998, but because of the under-estimation of fire
7 incidence mentioned before, the actual extent of that extreme fire episode is not captured.

8 [40] Next to each time series, the regional fire size distribution histograms for 2005 suggest the
9 representation of single fire size in HESFIRE is within the range of observations, and that it depicts
10 the decreasing fire frequency as a function of fire size. It tends to overestimate the frequency of
11 large fires and their contribution to the total burned area, however. Fire duration could not be
12 readily evaluated with the MODIS data, but a map of maximum fire duration is provided in
13 supplementary material to illustrate this capability (Figure S3). 68% of the 2005 burned area
14 occurred in fires longer than one day in HESFIRE.

15 **3.3. Model sensitivity**

16 [41] The sensitivity analysis shows the class of the parameter whose altered values (+50% and -
17 50%) led to the largest change in averaged annual burned area at the grid-cell level (Figure 8). In
18 boreal regions, although HESFIRE does not perform well, fire incidence is mostly sensitive to
19 weather parameters, and to a lower extent to the fuel load parameter. In humid tropical ecosystems,
20 HESFIRE is also mostly sensitive to weather parameters, but anthropogenic parameters become
21 dominant in areas with a substantial dry season and agricultural activities, especially in South
22 America along the arc of deforestation. In semi-arid areas, the vegetation fuel parameter has the
23 most influence, including in Mexico, sub-Saharan and southern sub-equatorial Africa, the horn of

1 Africa, Australia and Kazakhstan, with consequences for the model performance in these various
2 regions (see discussion). Finally, HESFIRE is primarily sensitive to the landscape fragmentation
3 parameter in several regions due to two mechanisms. In regions of high land use density (e.g. India),
4 fire spread is constantly limited by the fragmentation parameter and fire incidence is low, but can
5 increase (or diminish further) when altering its value. In regions of low land use density but high fire
6 incidence due to a very seasonal climatology (e.g. sub-Saharan and northern sub-equatorial Africa),
7 landscape fragmentation due to previous fires becomes a limiting factor for late-season fires. Finally,
8 regions of relatively high land use density and fire incidence are probably sensitive to both
9 mechanisms. Note that a landscape fragmentation is in part due to human activities, adding to the
10 sensitivity of the model to anthropogenic factors.

11 **4. Discussion**

12 **4.1. Model performance and potential improvements**

13 [42] HESFIRE shows encouraging capabilities, especially given the difficulty of achieving a good
14 representation of global fire patterns (Bowman et al., 2011; Spessa et al., 2013). It is a first step
15 towards the 3 objectives stated in introduction. First, the model avoids some assumptions that
16 would be fundamentally inconsistent with fire ecology (e.g. fire spread limited to a single day).
17 Second, it includes climatic, anthropogenic and vegetation drivers, and the input variables were
18 chosen so as to enable integration within dynamic vegetation and integrated assessment models (e.g.
19 human ignitions dependent on land use instead of population). Third, HESFIRE reproduces
20 reasonably well many aspects of regional fire activity, including fire incidence and variability in South
21 America and fire size, both of which were not part of the optimization procedure, and its regional
22 sensitivity to the 4 parameter classes corresponds to what would be expected based on broad fire
23 ecology concepts.

1 [43] The comparison to results reported by other models – mostly fire incidence – suggests
2 HESFIRE generally achieves strong performances on spatial patterns (Figure 6 in this paper, figure
3 3c in Thonicke et al., 2010, figure 2 in Prentice et al., 2011, figure 1 in Kloster et al., 2010), and on
4 the actual quantification of the average burned area fraction, with a rather infrequent occurrence of
5 large discrepancies which are susceptible to severely bias impacts on vegetation and carbon
6 dynamics. Note however that these results are not fully comparable as they are produced from fire-
7 modules embedded within dynamic vegetation models, with potential bias originating from other
8 parts of the model (e.g. PFT distribution, fuel load). The fire model developed by Li et al. (2012) and
9 modified to better account for anthropogenic ignitions has similar spatial patterns of averaged
10 burned area to HESFIRE (figure 9 in Li et al., 2013).

11 [44] The combination of these characteristics and performance suggests that the modeling and
12 optimization framework realistically captures the primary fire-driving mechanisms and the specific
13 magnitude of their influence regionally. It could thus bring relevant insights into future fire activity
14 under altered environmental conditions, including agricultural expansion and extreme climatic events
15 (e.g. sustained droughts). There are however a number of issues, as well as key potential
16 improvements which we discuss in the next sections.

17 **4.1.1. Fire incidence in boreal regions**

18 [45] HESFIRE under-estimates fire incidence in Boreal regions. This issue has been reported
19 before by Rupp et al. (2007), whose model projected almost no burned area when driven by the
20 NCEP data but performed better when driven by other datasets. Serreze and Hurst (2000) found
21 that summer precipitation is largely over-estimated in NCEP, compromising the whole hydrological
22 cycle including RH and soil moisture. Alternative datasets may address this issue, either by using

1 them as a direct input or to correct the bias in the NCEP data while maintaining its high temporal
2 resolution and extensive timespan.

3 [46] HESFIRE might be further limited because it does not represent specific aspects of boreal
4 fire regimes. In particular, boreal needle-leaf forests are highly flammable and have a vertical
5 structure favorable to the development of crown fires, which spread faster and can overcome higher
6 levels of moisture and humidity (Ryan, 2002). Additionally, large boreal fires typically spread over
7 weeks or months - which can be captured by HESFIRE - but might also remain dormant in a
8 smoldering phase during fire-averse conditions and re-activate later without any new ignitions
9 (Sedano and Randerson, 2014).

10 **4.1.2. Fires in semi-arid regions and links to the fuel proxy**

11 [47] Semi-arid ecosystems presented a particular challenge due to the sensitivity of fuel
12 characteristics to soil, precipitation and potential evapotranspiration conditions, which cannot be
13 fully captured by the cumulative precipitation proxy. In the final parameterization, HESFIRE is in
14 good agreement with observations in Australia, southern hemisphere Africa and Kazakhstan, but
15 over-estimates fire incidence in Mexico, the horn of Africa and semi-desert areas at the border of the
16 Sahara (Figure 8). Precipitation patterns in these xeric landscapes vary widely. Some semi-desert
17 regions have low amounts of precipitation year-round (Kazakhstan), while others have short rainy
18 seasons (sub-Saharan Africa). The optimization procedure favors one set of conditions, leading to
19 unequal performances across these regions.

20 [48] Clearly there are other potential factors contributing to this issue, but most of them are likely
21 related to fuel characteristics. The integration of HESFIRE within a vegetation model (Sect. 4.2.3)
22 will be important to provide dynamic and process-based estimates of fuel load, fuel structure and

1 fuel moisture (see Sect 4.2.3). In parallel, integrating observation-derived estimates of aboveground
2 biomass (Saatchi et al., 2011) as a fuel-proxy could improve performances while maintaining the
3 value of a standalone version of HESFIRE.

4 **4.1.3. Representation of anthropogenic ignitions**

5 [49] Modeling the global diversity of fire practices remains a significant challenge. HESFIRE
6 performs well in regions with a well-established anthropogenic footprint on fire regimes, even
7 though it is based on a simplistic representation of fire practices and suppression effort by necessity
8 to obtain a globally consistent initial approach. The timing and frequency of anthropogenic ignitions
9 are a complex aspect to represent in global models. In sub-Saharan Africa for example, local
10 populations are known to burn numerous small fires early in the dry season to fragment the
11 landscape and limit the occurrence of high-intensity late-season fires (Laris, 2002; Le Page et al.,
12 2010a). These fire management practices are not accounted for in HESFIRE, leading to a delayed
13 fire-peak month (by 1-3 months), and to an over-estimation of the average fire size. Beyond this
14 specific case, fire practices vary as a function of land use (e.g. agriculture, pastures), of land use
15 transitions (e.g. deforestation and post-clearing activities Morton et al., 2008), of land management
16 practices (fire prevention, fire suppression), and can also be due to arson or leisure activities (e.g.
17 campfire). For agricultural lands, fire practices can be very specific (clearing, pre-sowing, pre- and
18 post-harvest burns) and last for as little as a week to several months (Le Page et al., 2010a). Finally,
19 these practices vary at local to global scale according to environmental conditions, the availability of
20 alternatives to fires (e.g. fertilizer, pest control), national regulations, fire fighting capabilities, etc.
21 There is not much ground to believe fire practices will closely follow future GDP and land use
22 trends, but they are part of the equation. Research towards a better representation of broad classes
23 of fire practices is ongoing (Li et al., 2013), and, as mentioned in other studies, fire driver analysis on

1 longer time periods (e.g. with historical reconstruction, Mouillot and Field, 2005) would provide
2 further guidance.

3 **4.1.4. Representation of fire spread**

4 [50] The evaluation suggests the modeled average fire size is within the observed range, but
5 HESFIRE tends to overestimate the contribution of large fires, which could be linked to the
6 representation of fire spread as an idealized elliptic shape, similar to other global fire models. Burned
7 areas are typically patchy and the front line rarely remains unbroken around the perimeter of the fire,
8 especially in fragmented and uneven landscapes. Better accounting for these aspects could improve
9 models performances, for example with the implementation of a fragmentation feedback on the
10 fraction of the idealized elliptical shape that actually burns.

11 [51] Additionally, anthropogenic fire practices mentioned in Sect. 4.1.3 can have a substantial
12 footprint on fire size, including in regions where it is over-estimated by HESFIRE. In sub-Saharan
13 Africa for example, a better representation of small early dry-season burns as a fire management
14 practice would lead to a more realistic accounting of fire sizes and of the landscape fragmentation
15 feedback on late-season fire spread.

16 **4.2. Applications to environmental issues and for decision support.**

17 **4.2.1. Projection of future fire activity**

18 [52] Large scale policy decisions on agricultural production and climate mitigation will have
19 impacts on fire activity and might have to adapt in response, which global fire models could help
20 anticipate. Projections of agricultural lands point to a wide range of potential outcomes regarding
21 their expansion in natural ecosystems, depending among other factors on food demand,
22 technological developments and policies such as incentives for forest conservation (e.g. REDD) or

1 biofuels expansion (DeFries and Rosenzweig, 2010; Thomson et al., 2010; Tilman et al., 2011).
2 Given the sensitivity of fire activity to human presence in the landscape and to climate, it is essential
3 to anticipate the fire impacts of these scenarios, as well as the synergies and trade-offs with their
4 respective societal goals (e.g. climate mitigation, food security, biodiversity). An integrated
5 perspective is key to understand the interactions in play and to provide some level of confidence in
6 projections of fire regimes under altered environmental conditions (Bowman et al., 2009, 2011). We
7 believe HESFIRE as a standalone version can provide relevant insights on fire incidence and
8 variability under projections of future climate (Taylor et al., 2012), land use (Hurt et al., 2011) and
9 societal conditions (Van Vuuren et al., 2011), and on regional sensitivities.

10 **4.2.2. Integration to vegetation and socio-economic models**

11 [53] Beyond fire incidence and variability, fire impacts are of primary importance in multiple
12 contexts, including climate mitigation policies and the global carbon cycle (Le Page et al., 2013; van
13 der Werf et al., 2010), ecosystem dynamics across major biomes (Bond-Lamberty et al., 2007;
14 Cochrane, 2009), as well as pollution, health effects and a wide range of economic aspects (e.g.
15 Bowman et al., 2011; Calkin et al., 2005; Kochi et al., 2010; Sastry, 2002).

16 [54] First, impacts on ecosystem dynamics, the carbon cycle and other pollutant emissions can be
17 explored in fire models coupled to dynamic vegetation model (e.g. Thonicke et al., 2010). HESFIRE
18 is being implemented in the Ecosystem Demography model (ED, Moorcroft et al., 2001) which is
19 well adapted for fire impacts modeling because it tracks vegetation patches of different ages within a
20 grid-cell and the size and type of successional cohorts within each patch. Such characteristics are
21 essential to realistically estimate fire behavior (e.g. ladder fuel and crown versus understory fires), fire
22 intensity and combustion completeness, size and PFT dependent fire-induced mortality (Brando et
23 al., 2012), snags and downed-fuel decomposition rates (Chambers et al., 2000; Palace et al., 2008),

1 and post-fire regrowth dynamics (Balch et al., 2008; Bond-Lamberty et al., 2007; Goetz et al., 2007).
2 Vegetation models also enable a process-based representation of key fire drivers, especially fuel load
3 and fuel moisture that are otherwise estimated through proxy variables in HESFIRE (precipitation
4 and soil moisture).

5 [55] Second, the role of fires within the Human-Earth system needs to be explored within an
6 integrated framework to provide consistent scenarios of climate, ecosystems and society under
7 different environmental policy assumptions (Le Page et al., 2013). HESFIRE has been specifically
8 developed to this end, with anthropogenic input data commonly reported and projected by
9 integrated assessment models (land use and GDP). Recent developments to couple integrated
10 assessment models to process-based vegetation and climate models (Jones et al., 2013) enable the
11 simultaneous consideration of societal, vegetation and climate dynamics and how they feed back on
12 each other, without the need to exogenously specify input data from other models run under
13 potentially conflicting assumptions and forcing. Such a framework is particularly relevant to explore
14 fires and their interaction within the Human-Earth System.

15 **5. Conclusions**

16 [56] HESFIRE and its optimization procedure provide a relevant tool to explore certain aspects
17 of fire ecology and to anticipate potential changes in fire activity. We provide a first assessment of
18 the uncertainties attached to the parameters and the model sensitivity to the driving assumptions
19 they represent. We identify limitations and propose key developments to address the most
20 significant ones. Finally, we highlight potential research areas to better understand contemporary
21 and future fire activity, to support estimates of greenhouse gas emissions and ecosystem dynamics,
22 and to provide policy makers with insights into the consequences of potential economic and
23 environmental decisions.

6. References

1 Abatzoglou, J. T. and Kolden, C. A.: Relative importance of weather and climate on wildfire growth in interior
2 Alaska, *Int. J. Wildland Fire*, 20(4), 479–486, 2011.

4 Adler, R. F., Huffman, G. J., Chang, A., Ferraro, R., Xie, P. P., Janowiak, J., Rudolf, B., Schneider, U., Curtis, S.
5 and Bolvin, D.: The version-2 global precipitation climatology project (GPCP) monthly precipitation analysis (1979-
6 present), *Journal of Hydrometeorology*, 4(6), 1147–1167, 2003.

7 Allen, D. J. and Pickering, K. E.: Evaluation of lightning flash rate parameterizations for use in a global chemical
8 transport model, *Journal of Geophysical Research: Atmospheres* (1984–2012), 107, 4711,
9 doi:10.1029/2005JG000042, 2002.

10 Arora, V. K. and Boer, G. J.: Fire as an interactive component of dynamic vegetation models, *Journal of Geophysical Research: Biogeosciences* (2005–2012), 110, G02008, doi:10.1029/2005JG000042 Available at:
11 <http://www.agu.org/journals/jg/jg0504/2005JG000042/2005jg000042-t01.txt> (Accessed 5 June 2013), 2005.

13 Balch, J. K., Nepstad, D. C., Brando, P. M., Curran, L. M., Portela, O., de Carvalho, O. and Lefebvre, P.: Negative
14 fire feedback in a transitional forest of southeastern Amazonia, *Global Change Biology*, 14(10), 2276–2287, 2008.

15 Bond-Lamberty, B., Peckham, S. D., Ahl, D. E. and Gower, S. T.: Fire as the dominant driver of central Canadian
16 boreal forest carbon balance, *Nature*, 450(7166), 89–92, 2007.

17 Bontemps, S., Defourny, P., Bogaert, E. V., Arino, O., Kalogirou, V. and Perez, J. R.: GLOBCOVER 2009-Products
18 Description and Validation Report, [online] Available from: <http://www.citeulike.org/group/15400/article/12770349>
19 (Accessed 25 February 2014), 2011.

20 Bowman, D. M. J. S., Balch, J., Artaxo, P., Bond, W. J., Cochrane, M. A., D'Antonio, C. M., DeFries, R., Johnston,
21 F. H., Keeley, J. E., Krawchuk, M. A., Kull, C. A., Mack, M., Moritz, M. A., Pyne, S., Roos, C. I., Scott, A. C.,
22 Sodhi, N. S. and Swetnam, T. W.: The human dimension of fire regimes on Earth, *Journal of Biogeography*, 38(12),
23 2223–2236, doi:10.1111/j.1365-2699.2011.02595.x, 2011.

24 Bowman, D. M. J. S., Balch, J. K., Artaxo, P., Bond, W. J., Carlson, J. M., Cochrane, M. A., D'Antonio, C. M.,
25 DeFries, R. S., Doyle, J. C., Harrison, S. P., Johnston, F. H., Keeley, J. E., Krawchuk, M. A., Kull, C. A., Marston,
26 J. B., Moritz, M. A., Prentice, I. C., Roos, C. I., Scott, A. C., Swetnam, T. W., Werf, G. R. van der and Pyne, S. J.:
27 Fire in the Earth System, *Science*, 324(5926), 481–484, doi:10.1126/science.1163886, 2009.

28 Brando, P. M., Nepstad, D. C., Balch, J. K., Bolker, B., Christman, M. C., Coe, M. and Putz, F. E.: Fire-induced tree
29 mortality in a neotropical forest: the roles of bark traits, tree size, wood density and fire behavior, *Global Change
30 Biology*, 18, 630–641, 2012.

31 Calkin, D. E., Gebert, K. M., Jones, J. G. and Neilson, R. P.: Forest Service Large Fire Area Burned and
32 Suppression Expenditure Trends, 1970–2002, [online] Available at:
33 http://www.fs.fed.us/pnw/pubs/journals/pnw_2005_calkin001.pdf (Accessed 17 April 2014), 2005.

34 Cardoso, M. F., Hurtt, G. C., MOORE, B., NOBRE, C. A. and PRINS, E. M.: Projecting future fire activity in
35 Amazonia, *Global Change Biology*, 9(5), 656–669, 2003.

36 Chambers, J. Q., Higuchi, N., Schimel, J. P., Ferreira, L. V. and Melack, J. M.: Decomposition and carbon cycling
37 of dead trees in tropical forests of the central Amazon, *Oecologia*, 122(3), 380–388, 2000.

38 CIA: The world factbook 2009, Central Intelligence Agency, Washington, DC [online] Available from:
39 <https://www.cia.gov/library/publications/download/download-2009>, 2009.

40 Cochrane, M. A.: Fire, land use, land cover dynamics, and climate change in the Brazilian Amazon, *Tropical fire
41 ecology*, 389–426, 2009.

1 Cramer, W., Bondeau, A., Woodward, F. I., Prentice, I. C., Betts, R. A., Brovkin, V., Cox, P. M., Fisher, V., Foley,
2 J. A. and Friend, A. D.: Global response of terrestrial ecosystem structure and function to CO₂ and climate change:
3 results from six dynamic global vegetation models, *Global change biology*, 7(4), 357–373, 2001.

4 DeFries, R. and Rosenzweig, C.: Toward a whole-landscape approach for sustainable land use in the tropics, *PNAS*,
5 107(46), 19627–19632, doi:10.1073/pnas.1011163107, 2010.

6 Fetzer, E., McMillin, L. M., Tobin, D., Aumann, H. H., Gunson, M. R., McMillan, W. W., Hagan, D. E., Hofstadter,
7 M. D., Yoe, J. and Whiteman, D. N.: Airs/amsu/hsb validation, *Geoscience and Remote Sensing, IEEE Transactions*
8 on, 41(2), 418–431, 2003.

9 Flannigan, M., Stocks, B., Turetsky, M. and Wotton, M.: Impacts of climate change on fire activity and fire
10 management in the circumboreal forest, *Global Change Biology*, 15(3), 549–560, doi:10.1111/j.1365-
11 2486.2008.01660.x, 2009.

12 Giglio, L., Randerson, J. T. and van der Werf, G. R.: Analysis of daily, monthly, and annual burned area using the
13 fourth-generation global fire emissions database (GFED4): ANALYSIS OF BURNED AREA, *Journal of*
14 *Geophysical Research: Biogeosciences*, 118(1), 317–328, doi:10.1002/jgrg.20042, 2013.

15 Giglio, L., Randerson, J. T., van der Werf, G. R., Kasibhatla, P. S., Collatz, G. J., Morton, D. C. and DeFries, R. S.:
16 Assessing variability and long-term trends in burned area by merging multiple satellite fire products,
17 *Biogeosciences*, 7(3), 1171–1186, doi:10.5194/bg-7-1171-2010, 2010.

18 Gillett, N. P., Weaver, A. J., Zwiers, F. W. and Flannigan, M. D.: Detecting the effect of climate change on
19 Canadian forest fires, *Geophysical Research Letters*, 31, L18211, doi:10.1029/2004GL020876 Available at:
20 <http://onlinelibrary.wiley.com/doi/10.1029/2004GL020876/full> (Accessed 5 June 2013), 2004.

21 Goetz, S. J., Bunn, A. G., Fiske, G. J. and Houghton, R. A.: Satellite-observed photosynthetic trends across boreal
22 North America associated with climate and fire disturbance, *Proceedings of the National Academy of Sciences of*
23 *the United States of America*, 102(38), 13521–13525, doi:10.1088/1748-9326/2/4/045031, 2005.

24 Goetz, S. J., Mack, M. C., Gurney, K. R., Randerson, J. T. and Houghton, R. A.: Ecosystem responses to recent
25 climate change and fire disturbance at northern high latitudes: observations and model results contrasting northern
26 Eurasia and North America, *Environmental Research Letters*, 2(4), 045031, 2007.

27 Greenville, A. C., Dickman, C. R., Wardle, G. M. and Letnic, M.: The fire history of an arid grassland: the influence
28 of antecedent rainfall and ENSO, *Int. J. Wildland Fire*, 18(6), 631–639, 2009.

29 Hurtt, G., Chini, L., Frolking, S., Betts, R., Feddema, J., Fischer, G., Fisk, J., Hibbard, K., Houghton, R., Janetos,
30 A., Jones, C. D., Kindermann, G., Kinoshita, T., Goldewijk, K. K., Riahi, K., Shevliakova, E., Smith, S., Stehfest,
31 E., Thomson, A., Thornton, P., van Vuuren, D. P. and Wang, Y. P.: Harmonization of land-use scenarios for the
32 period 1500–2100: 600 years of global gridded annual land-use transitions, wood harvest, and resulting secondary
33 lands, *Climatic Change*, 109, 1–45, 2011.

34

35 Jones, A. D., Collins, W. D., Edmonds, J., Torn, M. S., Janetos, A., Calvin, K. V., Thomson, A., Chini, L. P., Mao,
36 J. and Shi, X.: Greenhouse Gas Policy Influences Climate via Direct Effects of Land-Use Change., *Journal of*
37 *Climate*, 26, 3657–3670, 2013.

38 Kanamitsu, M., Ebisuzaki, W., Woollen, J., Yang, S. K., Hnilo, J. J., Fiorino, M. and Potter, G. L.: Ncep-doe amip-ii
39 reanalysis (r-2), *Bulletin of the American Meteorological Society*, 83(11), 1631–1644, 2002.

40 Keeley, J. E. and Fotheringham, C. J.: Impact of past, present, and future fire regimes on North American
41 Mediterranean shrublands, in *Fire and climatic change in temperate ecosystems of the Western Americas*, pp. 218–
42 262, Springer. [online] Available from: http://link.springer.com/chapter/10.1007/0-387-21710-X_8 (Accessed 5
43 June 2013), 2003.

1 Kloster, S., Mahowald, N. M., Randerson, J. T. and Lawrence, P. J.: The impacts of climate, land use, and
 2 demography on fires during the 21st century simulated by CLM-CN, *Biogeosciences*, 9(1), 509–525,
 3 doi:10.5194/bg-9-509-2012, 2012.

4 Kloster, S., Mahowald, N. M., Randerson, J. T., Thornton, P. E., Hoffman, F. M., Levis, S., Lawrence, P. J.,
 5 Feddema, J. J., Oleson, K. W. and Lawrence, D. M.: Fire dynamics during the 20 th century simulated by the
 6 Community Land Model, *Biogeosciences*, 7(6), 1877–1902, 2010.

7 Kochi, I., Donovan, G. H., Champ, P. A. and Loomis, J. B.: The economic cost of adverse health effects from
 8 wildfire-smoke exposure: a review, *International journal of wildland fire*, 19(7), 803–817, 2010.

9 Korontzi, S., McCarty, J., Loboda, T., Kumar, S. and Justice, C.: Global distribution of agricultural fires in
 10 croplands from 3 years of Moderate Resolution Imaging Spectroradiometer (MODIS) data, *Global Biogeochemical
 11 Cycles*, 20, GB2021, doi:10.1029/2005GB002529, 2006.

12 Laris, P.: Burning the seasonal mosaic: preventative burning strategies in the wooded savanna of southern Mali,
 13 *Human Ecology*, 30(2), 155–186, 2002.

14 Li, F., Levis, S. and Ward, D. S.: Quantifying the role of fire in the Earth system-Part 1: Improved global fire
 15 modeling in the Community Earth System Model (CESM1),, *Biogeosciences*, 10(4) [online] Available from:
 16 <http://search.ebscohost.com/login.aspx?direct=true&profile=ehost&scope=site&authtype=crawler&jrnl=17264170&AN=87632324&h=i8QHQzgZ7%2FHjWJLViSy5RoSvuF1F83Nmnf8bcRueyXxmclkmUUpZdIsqqMePGLgwa9J%2FZy%2FIoZ8DMyqlmYUyDQ%3D%3D&crl=c> (Accessed 17 April 2014), 2013.

19 Li, F., Zeng, X. D. and Levis, S.: A process-based fire parameterization of intermediate complexity in a Dynamic
 20 Global Vegetation Model, *Biogeosciences*, 9(7), 2761–2780, doi:10.5194/bg-9-2761-2012, 2012.

21 Liu, Y., Goodrick, S. and Heilman, W.: Wildland fire emissions, carbon, and climate: Wildfire–climate interactions,
 22 *Forest Ecology and Management*, 317, 80–96, 2013.

23 Liu, Y., Stanturf, J. and Goodrick, S.: Trends in global wildfire potential in a changing climate, *Forest Ecology and
 24 Management*, 259(4), 685–697, 2010.

25 Metropolis, N., Rosenbluth, A. W., Rosenbluth, M. N., Teller, A. H. and Teller, E.: Equation of state calculations by
 26 fast computing machines, *The journal of chemical physics*, 21, 1087, doi:10.1063/1.1699114, 1953.

27 Moorcroft, P., Hurtt, G. and Pacala, S.: A method for scaling vegetation dynamics: the ecosystem demography
 28 model (ED), *Ecological Monographs*, 71(4), 557–586, 2001.

29 Morton, D. C., Defries, R. S., Randerson, J. T., Giglio, L., Schroeder, W. and van Der Werf, G. R.: Agricultural
 30 intensification increases deforestation fire activity in Amazonia, *Global Change Biology*, 14(10), 2262–2275, 2008.

31 Morton, D. C., Le Page, Y., DeFries, R., Collatz, G. J. and Hurtt, G. C.: Understorey fire frequency and the fate of
 32 burned forests in southern Amazonia, *Philosophical Transactions of the Royal Society B: Biological Sciences*, 368,
 33 doi:10.1098/rstb.2012.0163, 2013.

34 Mouillot, F. and Field, C. B.: Fire history and the global carbon budget: a $1^\circ \times 1^\circ$ fire history reconstruction for the
 35 20th century, *Global Change Biology*, 11(3), 398–420, doi:10.1111/j.1365-2486.2005.00920.x, 2005.

36 Mouillot, F., Schultz, M. G., Yue, C., Cadule, P., Tansey, K., Ciais, P. and Chuvieco, E.: Ten years of global burned
 37 area products from spaceborne remote sensing—A review: Analysis of user needs and recommendations for future
 38 developments, *International Journal of Applied Earth Observation and Geoinformation*, 26, 64–79,
 39 doi:10.1016/j.jag.2013.05.014, 2014.

40 Page, S. E., Siegert, F., Rieley, J. O., Boehm, H.-D. V., Jaya, A. and Limin, S.: The amount of carbon released from
 41 peat and forest fires in Indonesia during 1997, *Nature*, 420(6911), 61–65, 2002.

1 Le Page, Y., Hurtt, G., Thomson, A. M., Bond-Lamberty, B., Patel, P., Wise, M., Calvin, K., Kyle, P., Clarke, L.,
 2 Edmonds, J. and Janetos, A.: Sensitivity of climate mitigation strategies to natural disturbances, *Environmental*
 3 *Research Letters*, 8(1), 015018, doi:10.1088/1748-9326/8/1/015018, 2013.

4 Le Page, Y., Oom, D., Silva, J., Jönsson, P. and Pereira, J.: Seasonality of vegetation fires as modified by human
 5 action: observing the deviation from eco-climatic fire regimes, *Global Ecology and Biogeography*, 19(4), 575–588,
 6 2010a.

7 Le Page, Y., Pereira, J. M. C., Trigo, R., Camara, C. da, Oom, D. and Mota, B.: Global fire activity patterns (1996–
 8 2006) and climatic influence: an analysis using the World Fire Atlas, *Atmospheric Chemistry and Physics*, 8(7),
 9 1911–1924, 2008.

10 Le Page, Y., van der Werf, G., Morton, D. and Pereira, J.: Modeling fire-driven deforestation potential in Amazonia
 11 under current and projected climate conditions, *Journal of Geophysical Research*, 115, G03012,
 12 doi:10.1029/2009JG001190, 2010b.

13 Palace, M., Keller, M. and Silva, H.: Necromass production: studies in undisturbed and logged Amazon forests,
 14 *Ecological Applications*, 18(4), 873–884, 2008.

15 Parry, M. L.: *Climate Change 2007: Impacts, Adaptation and Vulnerability: Working Group II Contribution to the*
 16 *Fourth Assessment Report of the IPCC Intergovernmental Panel on Climate Change*, Cambridge University Press,
 17 2007.

18 Pechony, O. and Shindell, D. T.: Fire parameterization on a global scale, *Journal of Geophysical Research: Atmospheres* (1984–2012), 114, D16115, 2009.

20 Pereira, M. G., Trigo, R. M., da Camara, C. C., Pereira, J. M. C. and Leite, S. M.: Synoptic patterns associated with
 21 large summer forest fires in Portugal, *Agricultural and Forest Meteorology*, 129(1–2), 11–25,
 22 doi:10.1016/j.agrformet.2004.12.007, 2005.

23 Pfeiffer, M., Spessa, A. and Kaplan, J. O.: A model for global biomass burning in preindustrial time: LPJ-LMfire
 24 (v1.0), *Geosci. Model Dev.*, 6(3), 643–685, doi:10.5194/gmd-6-643-2013, 2013.

25 Podur, J., Martell, D. L. and Csillag, F.: Spatial patterns of lightning-caused forest fires in Ontario, 1976–1998,
 26 *Ecological Modelling*, 164(1), 1–20, doi:10.1016/S0304-3800(02)00386-1, 2003.

27 Potter, C. S., Wang, S., Nikolov, N. T., McGuire, A. D., Liu, J., King, A. W., Kimball, J. S., Grant, R. F., Frolking,
 28 S. E., Clein, J. S., Chen, J. M. and Amthor, J. S.: Comparison of boreal ecosystem model sensitivity to variability in
 29 climate and forest site parameters, *J. Geophys. Res.*, 106(D24), 33671–33687, doi:10.1029/2000JD000224, 2001.

30 Prentice, I. C., Kelley, D. I., Foster, P. N., Friedlingstein, P., Harrison, S. P. and Bartlein, P. J.: Modeling fire and
 31 the terrestrial carbon balance, *Global Biogeochemical Cycles*, 25, GB3005, doi:10.1029/2010GB003906, 2011.

32 Prentice, S. A. and Mackerras, D.: The ratio of cloud to cloud-ground lightning flashes in thunderstorms, *Journal of*
 33 *Applied Meteorology*, 16(5), 545–550, 1977.

34 Randerson, J., Liu, H., Flanner, M., Chambers, S., Jin, Y., Hess, P., Pfister, G., Mack, M., Treseder, K., Welp, L. R.,
 35 Chapin, F. S., Harden, J. W., Goulden, M. L., Lyons, E., Neff, J. C., Schuur, E. A., and Zender, C. S.: The impact of
 36 boreal forest fire on climate warming, *Science*, 314(5802), 1130–1132, 2006.

37 Rienecker, M. M., Suarez, M. J., Gelaro, R., Todling, R., Bacmeister, J., Liu, E., Bosilovich, M. G., Schubert, S. D.,
 38 Takacs, L., Kim, G.-K., Bloom, S., Chen, J., Collins, D., Conaty, A., da Silva, A., Gu, W., Joiner, J., Koster, R. D.,
 39 Lucchesi, R., Molod, A., Owens, T., Pawson, S., Pégion, P., Redder, C. R., Reichle, R., Robertson, F. R., Ruddick,
 40 A. G., Sienkiewicz, M. and Woollen, J.: MERRA: NASA's Modern-Era Retrospective Analysis for Research and
 41 Applications, *Journal of Climate*, 24(14), 3624–3648, doi:10.1175/JCLI-D-11-00015.1, 2011.

1 Roy, D. P., Boschetti, L., Justice, C. O. and Ju, J.: The collection 5 MODIS burned area product—Global evaluation
2 by comparison with the MODIS active fire product, *Remote Sensing of Environment*, 112(9), 3690–3707, 2008.

3 Running, S. W.: Ecosystem disturbance, carbon, and climate, *Science*, 321(5889), 652–653, 2008.

4 Rupp, T. S., Xi Chen, Olson, M. and McGuire, A. D.: Sensitivity of Simulated Boreal Fire Dynamics to
5 Uncertainties in Climate Drivers, *Earth Interactions*, 11(1), 1–21, 2007.

6 Ryan, K. C.: Dynamic interactions between forest structure and fire behavior in boreal ecosystems, *Silva Fennica*,
7 36(1), 13–39, 2002.

8 Saatchi, S. S., Harris, N. L., Brown, S., Lefsky, M., Mitchard, E. T. A., Salas, W., Zutta, B. R., Buermann, W.,
9 Lewis, S. L., Hagen, S., Petrova, S., White, L., Silman, M. and Morel, A.: Benchmark map of forest carbon stocks in
10 tropical regions across three continents, *PNAS*, 108(24), 9899–9904, doi:10.1073/pnas.1019576108, 2011.

11 Saltelli, A., Tarantola, S. and Campolongo, F.: Sensitivity Analysis as an Ingredient of Modeling, *Statistical
12 Science*, 15(4), 377–395, 2000.

13 Sastry, N.: Forest fires, air pollution, and mortality in Southeast Asia, *Demography*, 39(1), 1–23,
14 doi:10.1353/dem.2002.0009, 2002.

15 Scott, J. H. and Burgan, R. E.: Standard fire behavior fuel models: a comprehensive set for use with Rothermel's
16 surface fire spread model, *Gen. Tech. Rep. RMRS-GTR-153m* Fort Collins, CO: U.S. Department of Agriculture,
17 Forest Service, Rocky Mountain Research Station, 72p., 2005. Sedano, F. and Randerson, J. T.: Vapor pressure
18 deficit controls on fire ignition and fire spread in boreal forest ecosystems, *Biogeosciences Discussions*, 11(1),
19 1309–1353, doi:10.5194/bgd-11-1309-2014, 2014.

20 Serreze, M. C. and Hurst, C. M.: Representation of Mean Arctic Precipitation from NCEP–NCAR and ERA
21 Reanalyses., *Journal of Climate*, 13(1), 182–201, 2000.

22 Sitch, S., Smith, B., Prentice, I. C., Arneth, A., Bondeau, A., Cramer, W., Kaplan, J. O., Levis, S., Lucht, W., Sykes,
23 M. T., Thonicke, K. and Venevsky, S.: Evaluation of ecosystem dynamics, plant geography and terrestrial carbon
24 cycling in the LPJ dynamic global vegetation model, *Global Change Biology*, 9(2), 161–185, doi:10.1046/j.1365-
25 2486.2003.00569.x, 2003.

26 Soares-Filho, B., Silvestrini, R., Nepstad, D., Brando, P., Rodrigues, H., Alencar, A., Coe, M., Locks, C., Lima, L.,
27 Hissa, L., and Stickler, C. H.: Forest fragmentation, climate change and understory fire regimes on the Amazonian
28 landscapes of the Xingu headwaters, *Landscape ecology*, 27, 585–598, 2012.

29 Spearman, C.: The proof and measurement of association between two things, *The American journal of psychology*,
30 15(1), 72–101, 1904.

31 Spessa, A., van der Werf, G., Thonicke, K., Gomez Dans, J., Lehsten, V., Fisher, R. and Forrest, M.: Modeling
32 vegetation fires and fire emissions, in *Vegetation Fires and Global Change – Challenges for Concerted International
33 Action. A White Paper directed to the United Nations and International Organizations*, edited by J. G. Goldammer,
34 pp. 181–207, Kessel. [online] Available from: <http://www.forestrybooks.com> (Accessed 19 September 2014), 2013.

35 Stocker, T. F., Dahe, Q. and Plattner, G.-K.: Climate Change 2013: The Physical Science Basis, Working Group I
36 Contribution to the Fifth Assessment Report of the Intergovernmental Panel on Climate Change. Summary for
37 Policymakers (IPCC, 2013) [online] Available from:
38 http://www.climatechange2013.org/images/report/WG1AR5_Frontmatter_FINAL.pdf (Accessed 28 February
39 2014), 2013.

40 Stocks, B. J., Mason, J. A., Todd, J. B., Bosch, E. M., Wotton, B. M., Amiro, B. D., Flannigan, M. D., Hirsch, K. G.,
41 Logan, K. A., Martell, D. L. and Skinner, W. R.: Large forest fires in Canada, 1959–1997, *J. Geophys. Res.*,
42 107(D1), 8149, doi:10.1029/2001JD000484, 2002.

1 Taylor, K. E., Stouffer, R. J. and Meehl, G. A.: An overview of CMIP5 and the experiment design, *Bulletin of the*
2 *American Meteorological Society*, 93(4), 485–498, 2012.

3 Thomson, A. M., Calvin, K. V., Chini, L. P., Hurtt, G., Edmonds, J. A., Bond-Lamberty, B., Frolking, S., Wise, M.
4 A. and Janetos, A. C.: Climate mitigation and the future of tropical landscapes, *PNAS*, 107(46), 19633–19638,
5 doi:10.1073/pnas.0910467107, 2010.

6 Thonicke, K., Spessa, A., Prentice, I. C., Harrison, S. P., Dong, L. and Carmona-Moreno, C.: The influence of
7 vegetation, fire spread and fire behaviour on biomass burning and trace gas emissions: results from a process-based
8 model, *Biogeosciences*, 7(6), 1991–2011, 2010.

9 Thonicke, K., Venevsky, S., Sitch, S. and Cramer, W.: The Role of Fire Disturbance for Global Vegetation
10 Dynamics: Coupling Fire into a Dynamic Global Vegetation Model, *Global Ecology and Biogeography*, 10(6), 661–
11 677, doi:10.2307/3182693, 2001.

12 Thrupp, L. A., Hecht, S., Browder, J. O. and Institute, W. R.: The diversity and dynamics of shifting cultivation:
13 myths, realities, and policy implications, *World Resources Institute*., 1997.

14 Tilman, D., Balzer, C., Hill, J. and Befort, B. L.: Global food demand and the sustainable intensification of
15 agriculture, *PNAS*, 108(50), 20260–20264, doi:10.1073/pnas.1116437108, 2011.

16 Van Vuuren, D. P., Edmonds, J., Kainuma, M., Riahi, K., Thomson, A., Hibbard, K., Hurtt, G. C., Kram, T., Krey,
17 V. and Lamarque, J.-F.: The representative concentration pathways: an overview, *Climatic Change*, 109(1-2), 5–31,
18 2011.

19 Van der Werf, G. R., Dempewolf, J., Trigg, S. N., Randerson, J. T., Kasibhatla, P. S., Giglio, L., Murdiyarso, D.,
20 Peters, W., Morton, D. C. and Collatz, G. J.: Climate regulation of fire emissions and deforestation in equatorial
21 Asia, *Proceedings of the National Academy of Sciences*, 105(51), 20350–20355, 2008.

22 Van der Werf, G. R., Randerson, J. T., Giglio, L., Collatz, G., Mu, M., Kasibhatla, P. S., Morton, D. C., DeFries, R.,
23 Jin, Y. and van Leeuwen, T. T.: Global fire emissions and the contribution of deforestation, savanna, forest,
24 agricultural, and peat fires (1997–2009), *Atmos. Chem. Phys*, 10(23), 11707–11735, 2010.

25 Westerling, A. L., Cayan, D. R., Brown, T. J., Hall, B. L. and Riddle, L. G.: Climate, Santa Ana winds and autumn
26 wildfires in southern California, *Eos, Transactions American Geophysical Union*, 85(31), 289–296, 2004.

27 White, M. A., Thornton, P. E., Running, S. W. and Nemani, R. R.: Parameterization and Sensitivity Analysis of the
28 BIOME–BGC Terrestrial Ecosystem Model: Net Primary Production Controls, *Earth Interact.*, 4(3), 1–85,
29 doi:10.1175/1087-3562(2000)004<0003:PASAOT>2.0.CO;2, 2000.

30 Van Wilgen, B. w., Govender, N., Biggs, H. c., Ntsala, D. and Funda, X. n.: Response of Savanna Fire Regimes to
31 Changing Fire-Management Policies in a Large African National Park, *Conservation Biology*, 18(6), 1533–1540,
32 doi:10.1111/j.1523-1739.2004.00362.x, 2004.

33 Zaehle, S. and Friend, A. D.: Carbon and nitrogen cycle dynamics in the O-CN land surface model: 1. Model
34 description, site-scale evaluation, and sensitivity to parameter estimates, *Global Biogeochem. Cycles*, 24(1),
35 GB1005, doi:10.1029/2009GB003521, 2010.

36

37 **Acknowledgments:** The authors are grateful for research support provided by the NASA
38 Terrestrial Ecology and Inter-Disciplinary Studies programs. The authors also wish to express

1 appreciation to the Integrated Assessment Research Program in the Office of Science of the U.S.
2 Department of Energy for partially funding this research. The Pacific Northwest National
3 Laboratory is operated for DOE by Battelle Memorial Institute under contract DE-AC05-
4 76RL01830. The views and opinions expressed in this paper are those of the authors alone.

5

6 **Author contribution:** Y.L.P. developed the model and performed the simulations, Y.L.P.,
7 B.B.L. and G.H. designed the optimization procedure, Y.L.P. prepared the manuscript with
8 contribution from all authors.

1 **Table 1. Model parameters.**

Parameter	Description	Value & unit	Source [optimization range], if applicable
Ignitions			
CG _{ignp}	Cloud-to-Ground ignition probability . Average probability of ignition from a cloud-to-ground lightning strike on natural vegetation.	6.8%	Optimization [2.8 - 16.6]
LU _{ign}	Land Use ignitions . Original number of human ignitions per km ² of land use per 24 hour, prior to applying density-decreasing function (see LU _{exp}).	2.3×10^{-3} km ⁻¹	Optimization [1.1 – 6] $\times 10^{-3}$
LU _{exp}	Land Use exponent . Shape parameter: Controls the decreasing contribution of incremental land use areas to human ignitions	14.9	Optimization [14.7 – 19.8]
GDP _{exp} ^a	GDP exponent . Shape parameter: Impact of GDP on ignitions, through land use practices.	1.28	Optimization [0.83 – 3.02]
LU _{range}	Land Use range . of fractional land use controlling human ignitions, with no ignitions beyond the upper bound.	[0 - 0.1]	Successive trials for reasonable exponent value ^b
GDP _{range}	GDP range . Range of regional GDP controlling fire ignitions, through land use practices.	[0 - 60000] \$.cap ⁻¹ .year ⁻¹	Observed range ^c
Spread			
BA _{frag}	Burned Area fragmentation . Delay before burned areas can burn again (given sufficient precipitation for fuel accumulation), meanwhile contributing to fragmentation.	8 months	Model performance trials ^d
Max _{forestrate}	Maximum forest fire spread rate .	0.28m.s ⁻¹	(Scott and Burgan, 2005)
Max _{shrubrate}	Maximum shrublands fire spread rate .	1.12m.s ⁻¹	(Scott and Burgan, 2005)
Max _{grassrate}	Maximum grasslands fire spread rate .	2.79m.s ⁻¹	(Scott and Burgan, 2005)

RH_{range}	RH range. Range of relative humidity controlling fire spread.	[30 - 80]%	(Li et al., 2012) Scatter plot ^e Model performance trials
RH_{exp}	RH exponent. Shape parameter: Impact of relative humidity on fire spread rate.	1.18	Optimization [0.52 – 1.31]
SW_{range}	Soil Water range. Range of volumetric soil moisture controlling fire spread.	[20 - 35]%	Scatter plot Model performance trials
SW_{exp}	Soil Water exponent. Shape parameter: Impact of volumetric soil moisture on fire spread rate.	1.21	Optimization [0.30 – 1.44]
T_{range}	Temperature range. Range of temperature controlling fire spread.	[0 - 30]°C	Scatter plot Model performance trials
T_{exp}	Temperature exponent. Shape parameter: Impact of air temperature on fire spread rate.	1.78	Optimization [0.8 – 3.8]

Termination

$Fuel_{range}$	Fuel range. Range of precipitation controlling termination probability, through fuel build-up.	[0.5 - 3] mm.day ⁻¹	Scatter plot Model performance trials
$Fuel_{span}$	Fuel accumulation timespan. Timespan of average precipitation controlling fuel build-up.	12 months	(Greenville et al., 2009; Van der Werf et al., 2008; Van Wilgen et al., 2004) Model performance trials
$Fuel_{delay}$	Fuel accumulation delay. Delay from actual precipitation to fuel build-up.	3 months	Model performance trials
$Fuel_{exp}$	Fuel exponent. Shape parameter: Impact of precipitation over -15 to -3 months on fire termination probability, a proxy fuel build-up.	1.72	Optimization [1.62 – 3.65]
$Frag_{range}$	Fragmentation range. Range of fractional landscape fragmentation controlling termination probability.	[0 - 1]	Oberved range
$Frag_{exp}$	Fragmentation exponent. Shape parameter: Impact of landscape fragmentation on fire termination probability.	1.81	Optimization [0.94 – 2.48]

LU _{range}	Land Use range. Range of fractional land use controlling termination probability, through suppression efforts.	[0 - 0.1]	Successive trials for reasonable exponent value
LUSUP _{exp}	Land Use SUPpression exponent. Shape parameter: Impact of land use on fire termination probability, through suppression efforts, in interaction with GDP (below).	4.08	Optimization [1.62 – 7.18]
GDP _{range}	GDP range. Range of regional GDP controlling fire suppression effort.	[0 - 60000] \$.cap ⁻¹ .year ⁻¹	Oberved range
GDP _{exp} ^a	GDP exponent. Shape parameter: Impact of GDP on suppression effort, through land use practices.	1.28	Optimization [0.83 – 3.02]

1 ^a: in order to limit the number of parameters to optimize for the first version of the fire model, GDP_{exp} is attributed the same optimized
 2 value whether it applies to fire ignitions or fire termination.

3 ^b: Successive trials for reasonable exponent value. This was applied to the range of land use fraction for ignition and suppression (see
 4 Sect. 2.2.1.2).

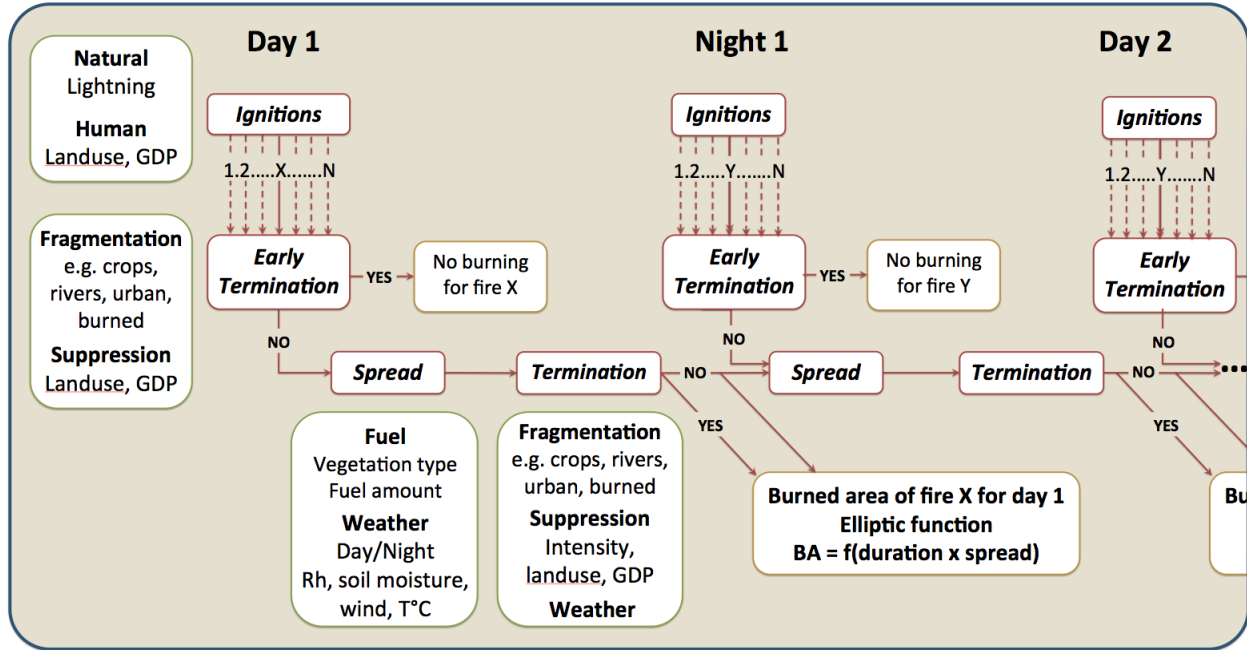
5 ^c: Oberved range. The range covers all or most of the values across the world. For GDP_{range}, a few grid-cells are beyond the
 6 60000\$/capita upper limit (in Qatar).

7 ^d: Model performance trials. These parameters were not determined using the full optimization procedure, but we tried a limited
 8 number of values (e.g. 5, 8 and 12 month for BA_{frag}) and selected the one leading to the best fit.

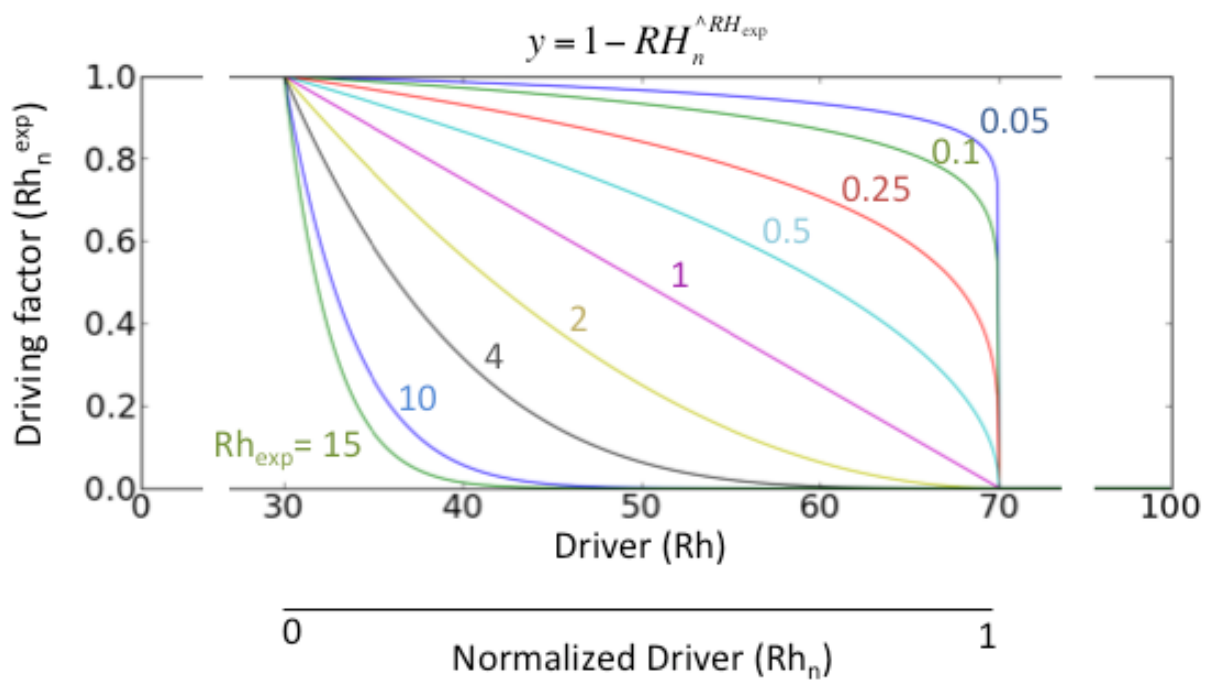
9 ^e: Scatter plot. We used scatter plot to determine the range of influence of some drivers, namely RH, soil moisture, temperature and the
 10 precipitation fuel proxy. An example is given in supplementary material.

11

1 **FIGURES**



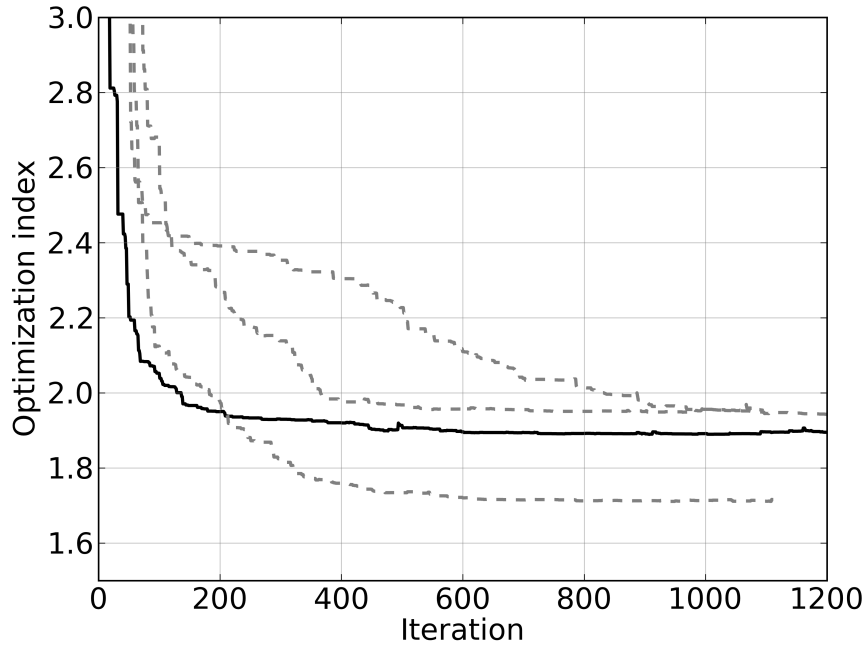
2 **Figure 1. HESFIRE diagram.**



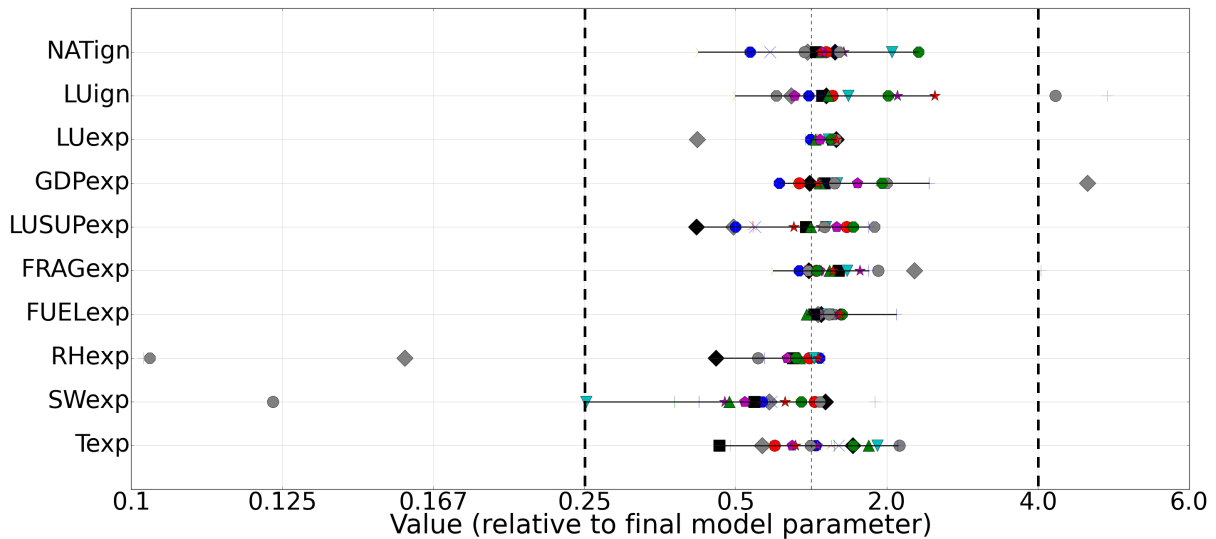
5 **Figure 2. Control of shape parameters (exponents, here RH_{exp}) on fire driving relationships.**

6 The exponent can take any value (from 0.033 to 30) as determined by the optimization

7 procedure, thus covering a wide space of potential fire-driving influence.



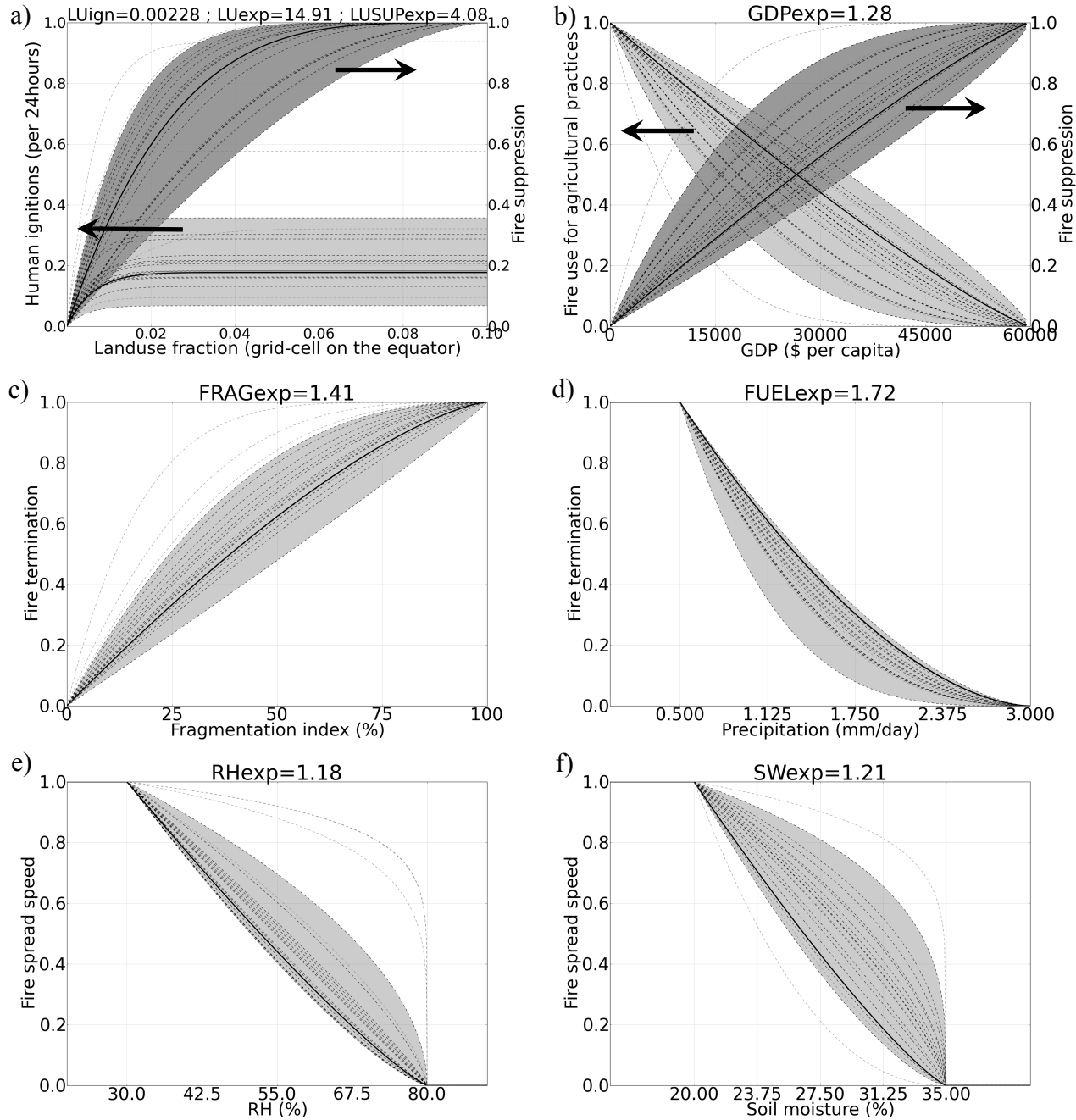
1
2 **Figure 3.** HESFIRE's performance through the optimization procedure iterations. The solid
3 line represents the optimization of the final model (which happened to reach a near-final
4 parameterization quite rapidly). The dashed lines represent the optimization of three of the
5 alternative runs, using different sets of grid-cells and years to evaluate the robustness of the
6 parameters.

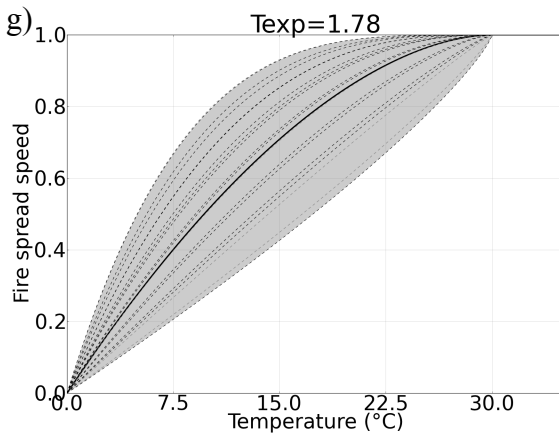


8
9 **Figure 4.** Parameter variability across the set of optimization runs with different grid-cells
10 and years. Among the 20 runs, 16 reached a relatively consistent parameterization (see text).
11 These are represented as colored markers and their range is shown by the black lines. For
12 the other 4 runs, parameters are shown as grey markers. The vertical dashed lines indicate
13 the lower and upper (symmetric) thresholds of parameters range that were used to separate
14 these 4 runs.

$$CG_{ignp} = 6.8\%$$

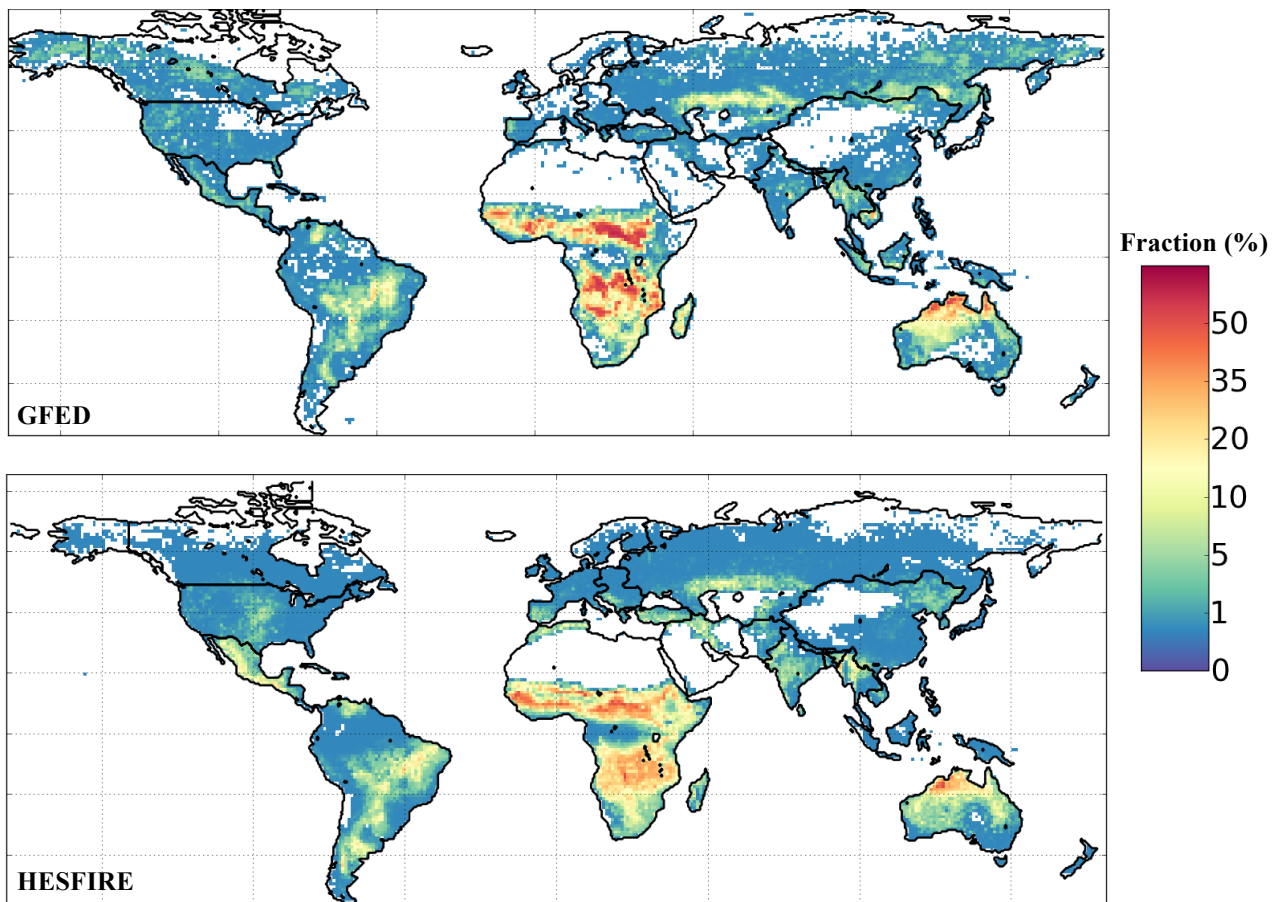
6.8% of cloud-to-ground lightning strikes on fire prone vegetation do ignite a fire. The range is 2.8% to 16.6% for the 16 optimization runs reaching a similar overall parameterization.



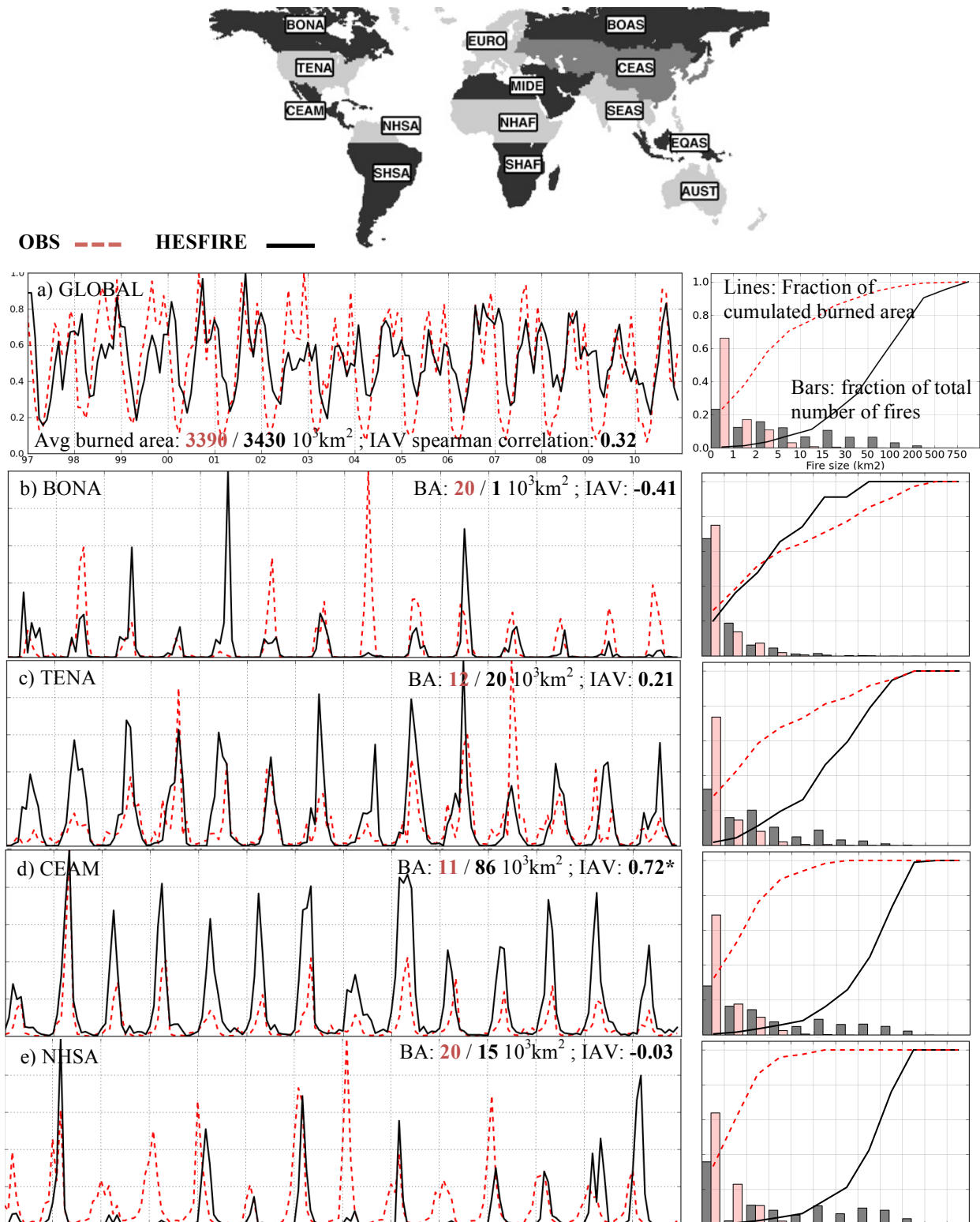


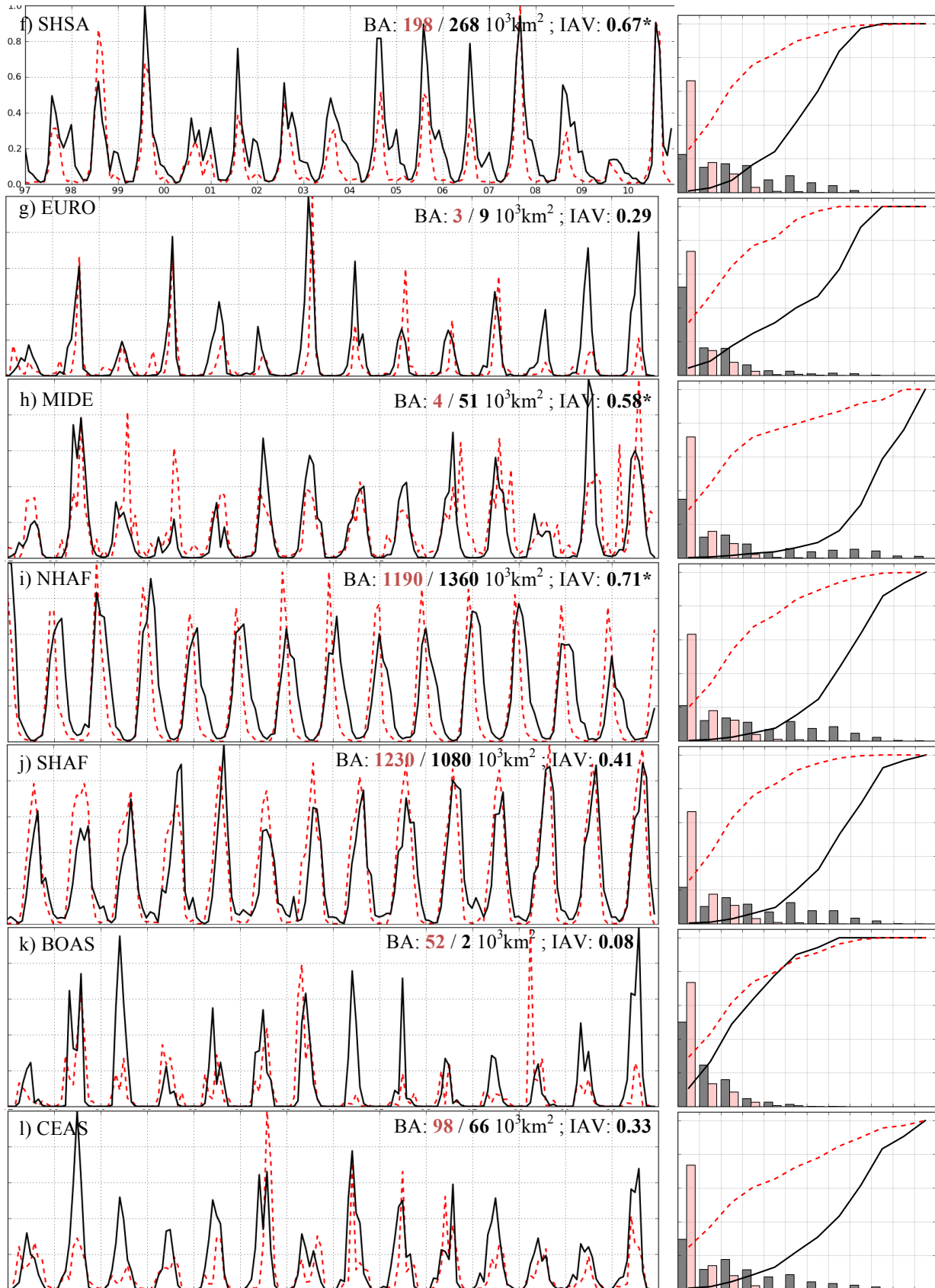
1 **Figure 5. Optimized model parameters and their influence on fire ecology.** For each plot,
 2 the thick black line represents the parameter influence in the final model. The dotted black
 3 lines represent the 16 optimization runs that reached a similar parameterization to the final
 4 model, the shaded area showing the range of their influence. The dotted grey lines represent
 5 the four optimization runs that reached a parameterization substantially different from the
 6 final model (see text).

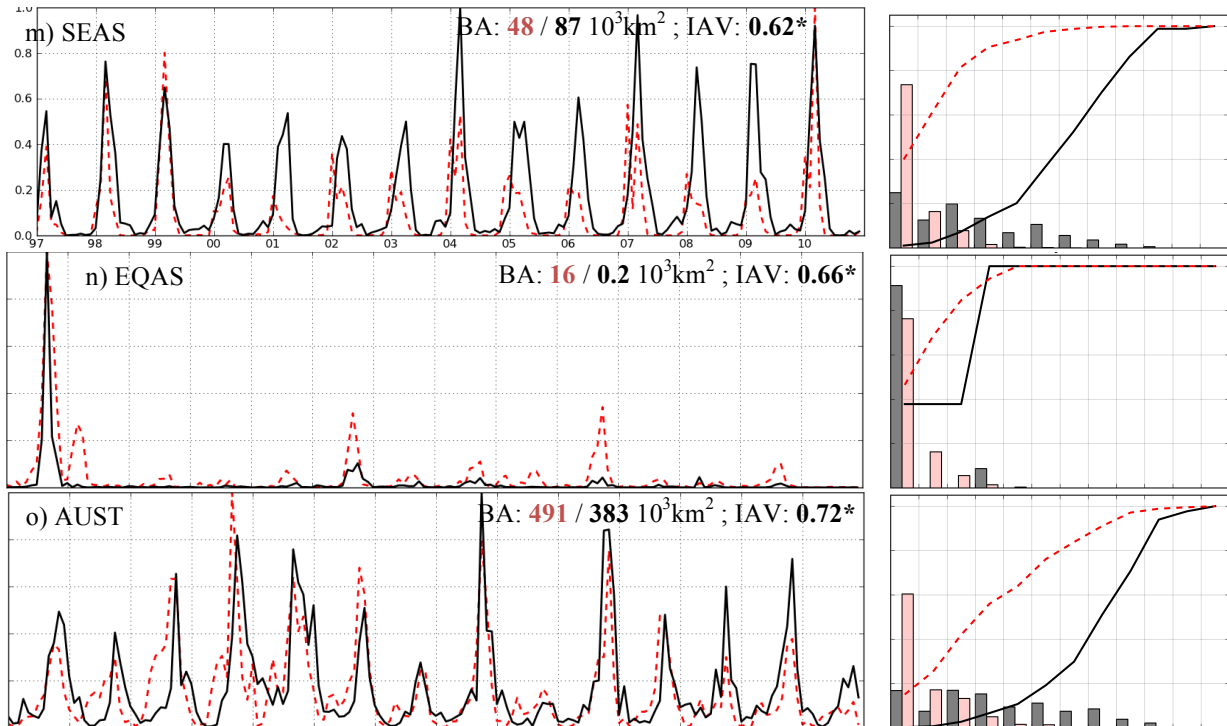
7



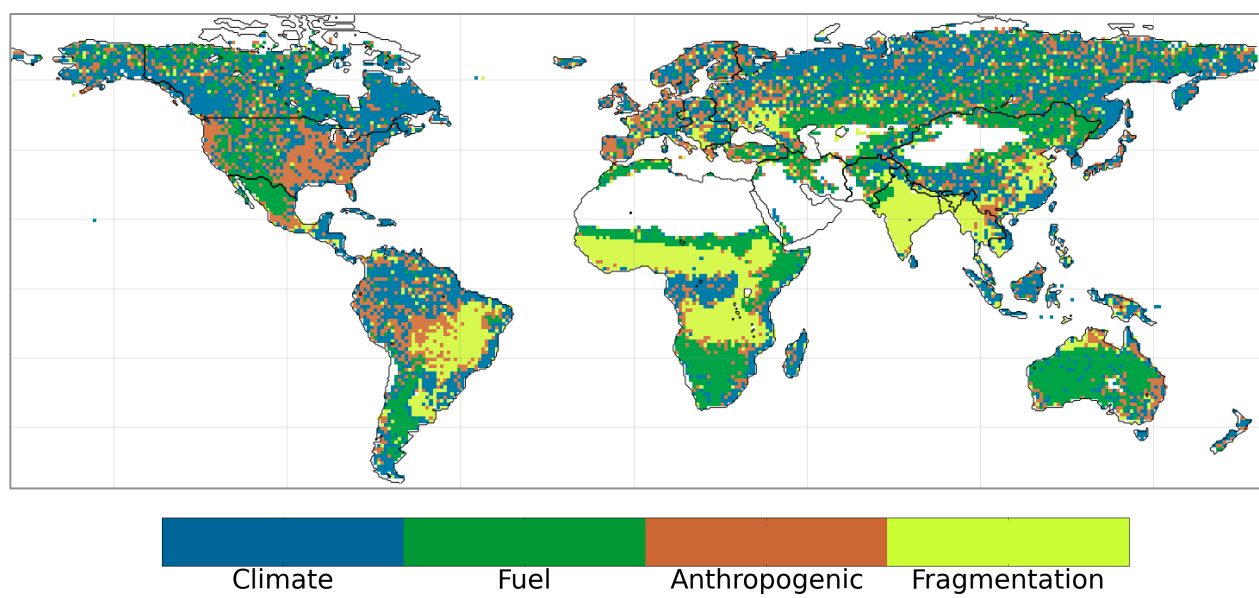
8 **Figure 6: Observed and modeled average annual burned fraction.** Top: GFEDv3 burned
 9 areas on “natural” landscapes. Bottom: Fire model.







1 Figure 7. Comparison of HESFIRE with observation-derived data over 14 regions. Left side
 2 plots: time series of normalized monthly burned area, with quantification of average annual
 3 burned area in GFED and in HESFIRE, and inter-annual correlation. Right side: 2005
 4 distribution of fires by size classes and cumulative burned area along these classes.
 5 Observation data are from the MODIS MCD45 product. * indicates significance of the IAV
 6 spearman correlation ($p < 0.05$, (Spearman, 1904))



10 Figure 8. Major drivers of average annual burned area sensitivity among the 9 optimized
 11 parameters as grouped into 4 thematic classes (climate, vegetation fuel, anthropogenic
 12 practices, landscape fragmentation). For each of the 9 parameters, HESFIRE was run
 13 keeping the original parameterization, but altering the value of the considered parameter by

1 -50% and +50%. The map shows the class of the parameter for which the average burned
2 area in the considered grid-cell varied the most between the 2 runs with these alternative
3 values.